

A genetic basis for facultative parthenogenesis in *Drosophila*

Highlights

- Parthenogenetic *D. mercatorum* displays genomic and transcriptomic signatures
- A genetic cause underlies facultative parthenogenesis in drosophilids
- Facultative parthenogenesis can be genetically induced in *D. melanogaster*
- Induced parthenogenesis can result in polyploid *D. melanogaster*

Authors

Alexis L. Sperling, Daniel K. Fabian, Erik Garrison, David M. Glover

Correspondence

alb84@cam.ac.uk (A.L.S.),
dmglover@caltech.edu (D.M.G.)

In brief

Sperling et al. demonstrate that facultative parthenogenesis can be engineered in the non-parthenogenetic *D. melanogaster* by manipulating candidate genes identified in the naturally parthenogenetic *D. mercatorum*. The resulting heritable neo-parthenogenesis therefore identifies a genetic basis for facultative parthenogenesis in *Drosophila*.

Article

A genetic basis for facultative parthenogenesis in *Drosophila*

Alexis L. Sperling,^{1,4,6,*} Daniel K. Fabian,¹ Erik Garrison,² and David M. Glover^{1,3,5,*}

¹University of Cambridge, Department of Genetics, Downing Street, Cambridge CB2 3EH, UK

²University of Tennessee Health Science Center, S Manassas Street, Memphis, TN 38103, USA

³Division of Biology and Biological Engineering, California Institute of Technology, East California Boulevard, Pasadena, CA 91125, USA

⁴Twitter: @AlexisLSperling

⁵Twitter: @LabGlover

⁶Lead contact

*Correspondence: alb84@cam.ac.uk (A.L.S.), dmglover@caltech.edu (D.M.G.)

<https://doi.org/10.1016/j.cub.2023.07.006>

SUMMARY

*Facultative parthenogenesis enables sexually reproducing organisms to switch between sexual and asexual parthenogenetic reproduction. To gain insights into this phenomenon, we sequenced the genomes of sexually reproducing and parthenogenetic strains of *Drosophila mercatorum* and identified differences in the gene expression in their eggs. We then tested whether manipulating the expression of candidate gene homologs identified in *Drosophila mercatorum* could lead to facultative parthenogenesis in the non-parthenogenetic species *Drosophila melanogaster*. This identified a polygenic system whereby increased expression of the mitotic protein kinase *polo* and decreased expression of a desaturase, *Desat2*, caused facultative parthenogenesis in the non-parthenogenetic species that was enhanced by increased expression of *Myc*. The genetically induced parthenogenetic *Drosophila melanogaster* eggs exhibit *de novo* centrosome formation, fusion of the meiotic products, and the onset of development to generate predominantly triploid offspring. Thus, we demonstrate a genetic basis for sporadic facultative parthenogenesis in an animal.*

INTRODUCTION

Parthenogenesis generates uniparental offspring with only the maternal genome; it is often a virgin birth. First observed in aphids by Charles Bonnet in the mid-18th century, it has since been found in almost every phylum. Facultative parthenogenesis permits the switch between sexual and parthenogenetic reproduction, whereas obligate parthenogens do not readily undertake sexual reproduction.^{1,2} In sexual reproduction, both sexes undertake meiosis to generate a complement of haploid cells or nuclei. One of these cells or nuclei combines with another from the opposite sex or mating type to generate a diploid zygote. Some parthenogenetic animals appear to bypass meiosis completely, and through *apomixis*, they proceed straight into mitosis, whereas most parthenogens retain key meiotic machinery and undergo *automixis*. Diploidy is either retained in *automixis* by genome duplication prior to meiosis or by skipping parts of meiosis or regained after meiosis by genome duplication or fusion of two haploid meiotic products. To date, potential mechanisms for parthenogenesis can only be inferred from the stage at which sexual reproduction is bypassed.

Parthenogenesis has evolved in many animal and plant phyla. However, although in most animals there is no requirement for complementary genetic contributions from the two parents, in mammals, sex-specific epigenetic marks direct the monoallelic, parent-specific expression of around 150 genes,^{3,4} preventing the development of embryos with only a maternal genome. A

parthenogenetic mouse has been made by selectively methylating or demethylating imprinted genes.⁵ Once activated, the resulting oocytes developed into blastocysts that were transferred to surrogate mothers, but despite re-establishing correct imprinting, the success rate was extremely low. This highlights the importance of correctly regulated parental genome expression and suggests that additional mechanisms may prevent parthenogenesis in mammals. The mouse is, however, one of the few vertebrate species that can initiate development without the contribution of a centriole from the sperm. Centrioles are eliminated from the eggs of most animals and thus must form *de novo* or be provided by the sperm basal body to enable embryonic cell divisions.^{6–8} Indeed, in the frog, the injection of purified centrosomes mimics fertilization and leads to parthenogenetic development of tadpoles.⁹

In contrast to the non-heritable parthenogenesis of the frog and mouse, many animals undertake natural heritable parthenogenesis if specific developmental requirements are met. Several potential genetic mechanisms for obligate parthenogenesis have been identified through gene expression and mapping studies, but none have been tested either because of genetic intractability of the specific organism or because the studies were carried out prior to the genome editing era. Obligate parthenogenesis has been associated with downregulation of a gene encoding a regulatory subunit of protein phosphatase 2A (PP2A), *twins*, in the ovarian tissue of water weevils¹⁰; reduced expression of cell-cycle genes¹¹ and suppressors of meiosis in

water fleas¹²; a microsatellite-associated allele in a parasitoid wasp¹³; and a gene putatively involved in chromosome segregation in the cape honeybee.¹⁴ A mutant gene causing inability to respond to chemical signals for sexual reproduction has been proposed to switch alternating cycles of sexual and parthenogenetic reproduction to obligate parthenogenesis in rotifers.¹⁵ Facultative parthenogenesis may offer an understanding of how obligate parthenogenesis first arises, but the only suggestion of its genetic cause is a monogenic change of unknown consequence on the second chromosome of *Drosophila ananassae*.¹⁶ More recently, comparative genomics has identified subsets of genes altered in parthenogenetic genomes.¹⁷ However, most comparative studies contrast obligate parthenogenetic lineages to sexually reproducing counterparts, which sometimes diverged millions of years ago. Thus, without functional testing, it becomes impossible to separate primary cause from downstream consequence.

We argued that because facultative parthenogenesis can undergo selection in *Drosophila*, locusts, and chickens and can increase in frequency over generations,^{18–21} it should be possible to uncover the underlying genetic cause. With this in mind, we sought to identify the genetic origins of facultative parthenogenesis in *Drosophila mercatorum* by sequencing its genome, comparing gene expression patterns in mature eggs of females undertaking sexual or parthenogenetic reproduction, and functionally testing candidate genes for their ability to transmit facultative parthenogenesis. In this way, we identify gene expression changes in *D. mercatorum* associated with parthenogenetic reproduction and show how altering the expression of these genes can cause a sexually reproducing species, *Drosophila melanogaster*, to undertake heritable facultative parthenogenesis.

RESULTS

Parthenogenetic ability of *D. mercatorum*

Uniquely, *D. mercatorum* strains show a range of sexual and parthenogenetic reproductive capabilities. Some wild-caught strains behave as obligate parthenogens that can be maintained in the lab indefinitely as female-only stocks, and most strains exhibit low levels of facultative parthenogenesis,^{21–23} whereas other strains reproduce predominantly sexually. *D. mercatorum* belongs to the *repleta* species group, which is approximately 47 Ma diverged from *D. melanogaster*.²⁴ Although most *repleta* species breed on cacti, some *D. mercatorum* strains have diversified their larval diet to include rotting food waste²⁵; this change in diet is linked to enhanced parthenogenesis.²⁶ We selected two strains to sequence from a series of *D. mercatorum* strains that could all interbreed (Data S1A): a fully parthenogenetic strain from Hawaii that generated 326.1% adult offspring (3.36 adult offspring per female) and a sexually reproducing strain that could not parthenogenetically generate adult offspring from São Paulo, Brazil (Figure 1A; Data S1B).

The genome of *D. mercatorum*

We first created chromosome-level genome assemblies for sexually reproducing and parthenogenetic strains of *D. mercatorum* using Oxford Nanopore and Illumina sequencing technologies (Figures 1B and S1A–S1C). The two *D. mercatorum*

genome assemblies were annotated using homology to *D. melanogaster* genes and were comparably complete in gene content, with BUSCO scores of 98% for the sexually reproducing and 99% for the parthenogenetic strain (Figures 1B and S1D). These two *D. mercatorum* genomes were aligned against the *D. melanogaster* genome benchmark (Figures 1C and S2A–S2D). The *D. mercatorum* contigs matched to single *D. melanogaster* chromosome arms, despite a high degree of rearrangement within the arms. This is a well-known phenomenon in *Drosophila* where the chromosome arms, also referred to as Muller elements A–F, carry a homologous gene set in a shuffled order.^{27–29} Using a fluorescence *in situ* hybridization chain reaction (HCR) protocol adapted for localizing DNA sequences, we identified selected loci and thus the chromosome arms in the diploid chromosome spreads of larval neuroblasts (Figure 1D). The loci correspond to single genes that lay within syntenic blocks conserved between *D. melanogaster* and *D. mercatorum* chromosome arms. The 6 Muller elements (A–F) in the mitotic karyotypes matched between the sexually reproducing and parthenogenetic *D. mercatorum* strains (Figure 1E).

We next aligned the sexually reproducing and parthenogenetic *D. mercatorum* genomes against each other and found them highly similar (Figures 1C and 2A). There were inversions in chromosome arm 2L/Muller element B of the parthenogenetic genome reflecting known inversions on the 2L in different *D. mercatorum* populations.^{30,31} We also positioned the 14 largest contigs on the polytene salivary gland chromosomes (Figures 2B and 2C), providing biological validation for the genome assemblies.

Transcriptome changes in facultative parthenogenesis

As defining parthenogenetic events occur in the mature egg, we anticipated that this would be reflected in gene expression changes between the ovaries of parthenogenetic and non-parthenogenetic flies. The mature egg (stage 14 egg chamber) is a giant cell arrested in meiosis, in which neither transcription, translation, nor transcript degradation takes place.^{32,33} We used RNA sequencing to characterize transcriptomes of mature eggs from sexually reproducing and parthenogenetic *D. mercatorum* strains. We compared these profiles with that of a facultative parthenogenetic strain that reproduces sexually but produced 10.7% adult offspring parthenogenetically when sexually isolated (Data S1B). The transcriptome profiles identified 7,656 genes expressed in mature eggs (Data S2A–S2H). Genes exhibiting different transcript levels were evenly distributed on the contigs relative to gene content and were not overrepresented on a single chromosome arm (Figures S3A and S3B). Gene ontology (GO) analysis revealed that differentially expressed genes represented pathways of redox reactions, immune function, wing disc growth, biosynthesis, proteolysis, and translation (Figure S3C), any of which may aid parthenogenesis, but without any clear biological theme with potential for its initiation. We did, however, find an increase in transcripts of many centriole/centrosome/microtubule-organizing genes in parthenogenetic eggs, including *Cp110*, *dgt5*, *Poc1*, *Cep97*, *CG42699*, and *Rcd4*, possibly reflecting long implicated roles of centrioles in parthenogenesis by organizing the cell division machinery.^{9,34,35} We also found changes in cell-cycle regulatory gene transcripts, *e(r)*, *c(2)M*, *CG13088*, *Asciz*, *msd1*, *Roc1a*, *toc*, *Nup107*,

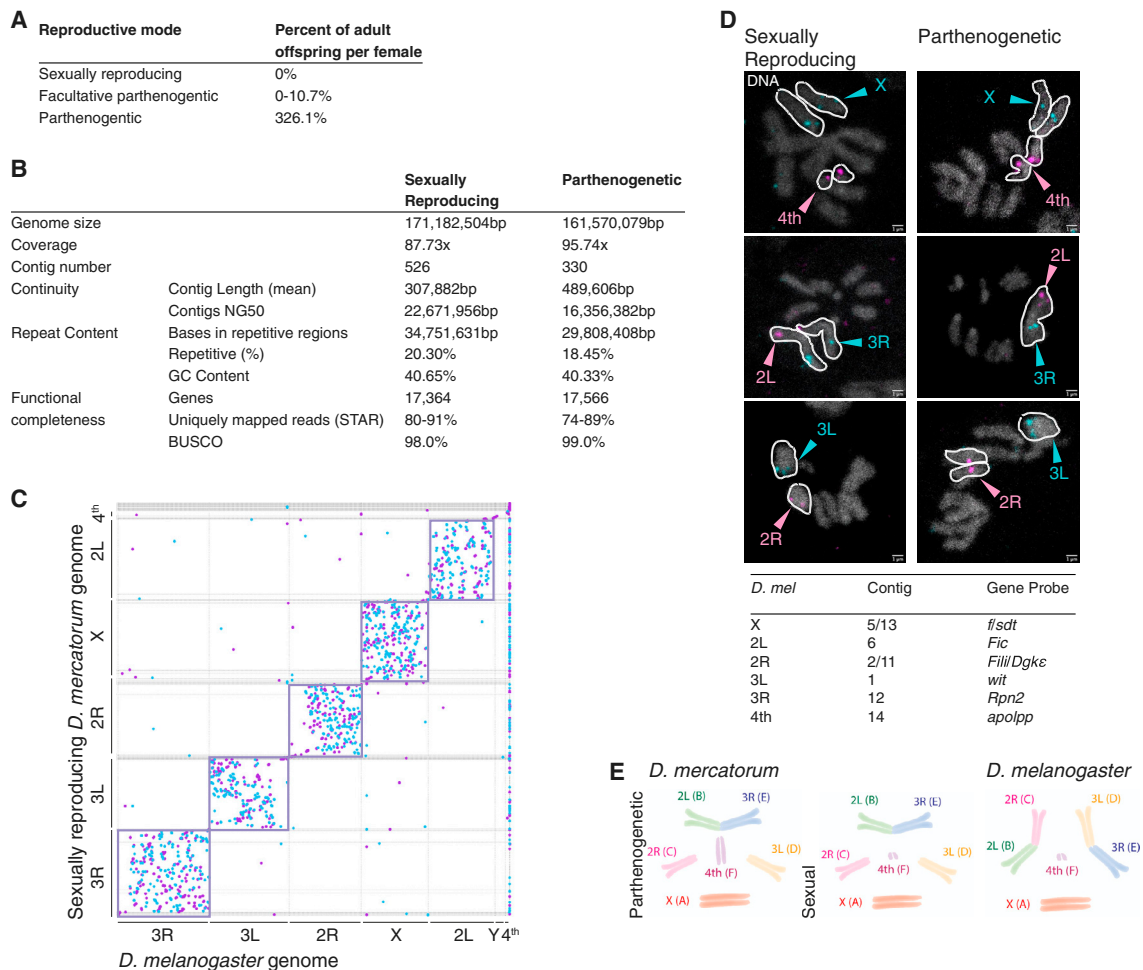


Figure 1. Comparison of sexually reproducing and parthenogenic *D. mercatorum* genomes to each other and *D. melanogaster*

(A) Reproductive modes of *D. mercatorum*.

(B) Sexually reproducing and parthenogenic *D. mercatorum* genome assembly data, quality control, and annotation metrics.

(C) Sexually reproducing *D. mercatorum* genome assembly aligned against the *D. melanogaster* reference genome (release 6). Alignment is over 75.28 Mbp, and the gap compressed identity is 75.85%. A raw version of this panel is presented in Figure S2A. Purple dots/lines represent sequences matching against the forward strand and blue the reverse.

(D) *In situ* localization of the indicated genes by HCR onto mitotic chromosomes of third instar larval neuroblasts from sexually reproducing and parthenogenic *D. mercatorum*. The karyotypes match except for a polymorphism in size for the 4th chromosome arm/Muller element F. Gene probes were selected to represent the indicated contigs. Chromosomes showing localization of the gene probe are outlined with a white line. The indicated chromosome was marked in all karyotypes analyzed ($n \geq 42$, $N \geq 3$). DAPI/DNA (white). Scale bars, 1 μ m.

(E) Schematic of the arrangement of the chromosome arms in sexually reproducing and parthenogenic strains of *D. mercatorum* and in *D. melanogaster*.

See also Figures S1 and S2 and Data S1.

CG33969, *mei-9*, CG31612, and *gnu*, in accordance with the need to activate cell-cycle progression in parthenogenic eggs. However, functional tests were required to relate such correlations with causal events of parthenogenesis. We therefore set thresholds of differential expression to approximate the loss or gain of one gene copy in the parthenogenic *D. mercatorum* eggs (p adjusted < 0.05; \log_2 -fold change \pm 0.6; Data S3A–S3D) and selected genes for functional testing with a focus on cell-cycle and centriole biogenesis (Figure S3D).

Functional screens for facultative parthenogenesis

We reasoned that if we could replicate the differential expression of homologous candidate genes in the strictly sexually

reproducing *Drosophila melanogaster* and induce facultative parthenogenesis in this species, this would provide strong evidence that such genes contribute to facultative parthenogenesis in the *Drosophila* genus. We first established a baseline for facultative parthenogenesis in different *Drosophila* species, including multiple *D. melanogaster* strains, to determine the number of flies that should be screened (Data S4A and S4B). We defined facultative parthenogenesis as permitting eggs produced by virgin mothers to develop from any stage between late embryogenesis and adulthood. We tested *D. melanogaster* homologs of genes having decreased expression in facultative and fully parthenogenic *D. mercatorum* eggs using CRISPR knockout alleles that we generated (Data S5), publicly available mutant

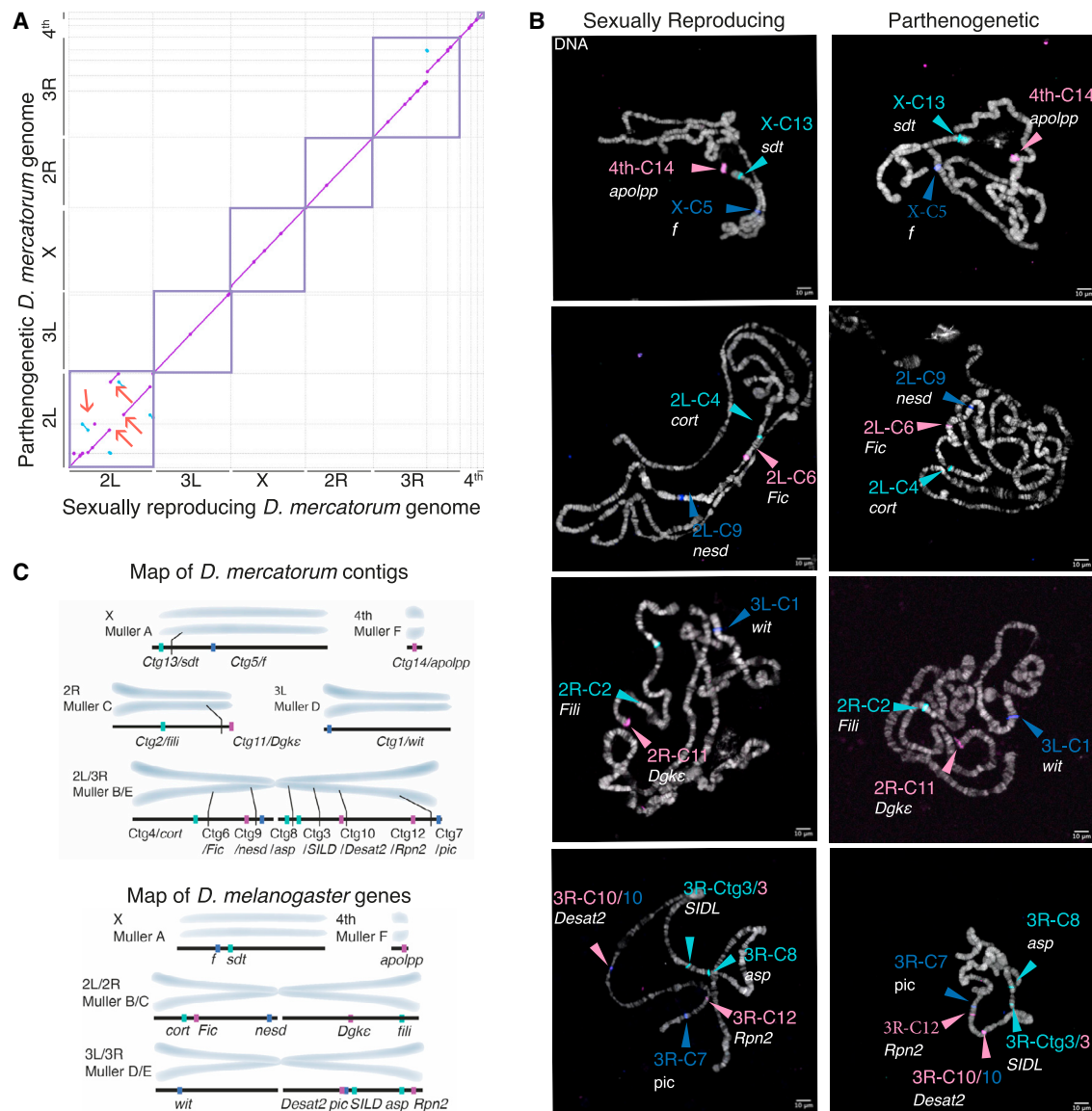


Figure 2. *D. mercatorum* genome comparison and physical mapping of the largest *D. mercatorum* contigs on polytene salivary gland chromosomes

(A) Alignment of the parthenogenetic *D. mercatorum* genome against the sexually reproducing genome. Red arrows indicate inversions/translocations. Alignment is over 151.14 Mbp, including 142.25 Mbp of matching base pairs. The gap compressed identity is 98.67%, while the “block” identity is 94.11%. The smallest contigs were removed from the visualization. Purple dots/lines represent sequences matching against the forward strand and blue the reverse strand.

(B) Mapping of the largest 14 contigs of the sexually reproducing and parthenogenetic *D. mercatorum* genomes onto salivary gland polytene chromosomes stained with DAPI. The contig and the chromosome arms are indicated with the arrows pointing to the HCR *in situ* hybridization band. These gene localizations show that the computationally assigned chromosome arms are appropriately grouped together in the biological samples. *In situ* hybridizations were carried out using the indicated HCR DNA probes corresponding to indicated genes. DNA/DAPI (white). Scale bars, 10 μ m.

(C) Schematic of mapping of the contigs onto *D. mercatorum* chromosomes and their corresponding positions on *D. melanogaster* chromosomes.

alleles, or established fly stocks carrying RNAi constructs to downregulate selected genes. RNAi lines were previously verified to have no known off-target effects (see links in [Data S6](#)). Genes showing increased expression in parthenogenetic *D. mercatorum* eggs were tested in *D. melanogaster* engineered to have increased expression of the homolog ([Table 1](#)). We also screened additional candidates with roles in the cell and centriole duplication cycles with the potential to generate diploid

nuclei from the haploid products of female meiosis or to offer a maternal source of centrioles in the absence of the sperm basal body upon fertilization, as thought to occur in *D. mercatorum* ([Table 1](#)).^{36,37} Rather than testing all differentially expressed genes regulating the centriole duplication cycles, we focused upon two main regulators of centrosome biogenesis, Polo-like kinase 4 (Plk4/SAK)³⁸ and Polo,³⁹ the latter also being a key regulator of cell-cycle progression.⁴⁰ As controls, we selected

Table 1. Candidate gene variants screened for ability to generate facultative parthenogenesis in *D. melanogaster*

Variant	Function	Log ₂ fold change	P _{adj}	Total offspring (%)	p value
Differentially expressed genes					
<i>Asciz</i> RNAi	transcription	−0.6	1.3 × 10 ^{−4}	0	1
<i>bam</i> RNAi/allele	cell fate	−4.8	8.4 × 10 ^{−25}		*
<i>c(2)M</i> RNAi	female meiosis	−1.4	1.7 × 10 ^{−8}	0	1
<i>Cad96Ca</i> RNAi	receptor tyrosine kinase	−7.4	2.5 × 10 ^{−126}	0	1
CASK deficiency	scaffolding	−0.8	2.2 × 10 ^{−5}	0	1
<i>tous</i> RNAi	cilia/flagella	−2.8	2.6 × 10 ^{−3}	0	1
CG4496 RNAi	transcription	−1.8	3.2 × 10 ^{−15}	*	1
CG10433 RNAi	female receptivity	−2.7	7.0 × 10 ^{−2}	*	0.4
CG17202 allele	Myc-binding	−0.8	3.5 × 10 ^{−5}	0	1
CG10407 RNAi	unknown	−3.4	N/A	2.5 × 10 ^{−3}	*
<i>chrb</i> RNAi	cell growth inhibition	−2.2	2.9 × 10 ^{−71}	*	1
CRMP RNAi/allele	pyrimidine catabolism	−3.0	5.2 × 10 ^{−4}	0%–0.2%	0.4–0.5
<i>Desat1</i> (<i>Desat2</i>) RNAi/allele	fatty acid desaturase	−0.6	0.17	0%–0.4%	1–3.5 × 10 ^{−2}
<i>Desat2</i> RNAi/allele	fatty acid desaturase	6.6	1.3 × 10 ^{−7}	0%–0.3%	0.4–1
<i>e(r)</i> allele	pyrimidine biosynthesis	−2.7	1.5 × 10 ^{−3}	0	1
<i>eya</i> OE	transcription	0.44	0.78	*	0.2–1
<i>f</i> RNAi/allele	actin filament	−2.8	3.7 × 10 ^{−11}	0%–0.1%	0.4–1
<i>FER</i> RNAi/allele	tyrosine kinase	−2.4	1.5 × 10 ^{−3}	0	0.4–1
<i>gnu</i> allele/OE	translation	3.5	1.7 × 10 ^{−73}	0%–0.2%	0.5–1
<i>ktub</i> RNAi/allele	endocytosis	−3.3	5.7 × 10 ^{−4}	0%–0.4%	0.2–1
<i>msd1</i> allele	mitotic spindle	−0.6	6.2 × 10 ^{−3}	0	1
<i>Myc</i> OE	transcription	0.7	9.2 × 10 ^{−3}	0.3%	0.1–0.5
<i>Nmnat</i> OE	adenyltransferase	1.7	1.9 × 10 ^{−10}	N/A	0
<i>pnt</i> OE	transcription	1.8	1.7 × 10 ^{−9}	0	1
<i>Rack1</i> allele	receptor	−0.7	1.3 × 10 ^{−2}	0.5%	0.06
<i>Rcd4</i> OE	centrosome	2.0	2.3 × 10 ^{−27}	N/A	0
<i>Roc1a</i> allele/OE	SCF complex/cell-cycle	−0.6	2.3 × 10 ^{−6}	*	1
<i>RpL10Ab</i> allele	ribosome	−0.8	1.6 × 10 ^{−8}	0	1
<i>spir</i> OE	actin nucleation	1.0	2.0 × 10 ^{−2}	0	1
Cell-cycle/centrosome candidate genes					
<i>ana2</i> CRISPR	centriole	N/A	N/A	0	1
<i>asl</i> CRISPR/OE	centriole/PCM	N/A	N/A	0%–0.1%	0.5–1
<i>cnn</i> allele	PCM	N/A	N/A	0.1%	0.5
<i>CycE</i> UAS/OE	cell cycle	N/A	N/A	0	1
<i>mtrm</i> allele	cell cycle	N/A	N/A	0	1
<i>morula</i> CRISPR	cell cycle	N/A	N/A	0%–0.1%	0.4–1
<i>Plp</i> CRISPR	PCM	N/A	N/A	0.1%	0.2
<i>plu</i> CRISPR	translation	N/A	N/A	0.1%	0.5–1
<i>png</i> CRISPR	translation	N/A	N/A	0	1
<i>polo</i> allele/OE	cell cycle	N/A	N/A	0%–0.1%	0.1–1
<i>Rca1</i> UAS/OE	cell cycle	N/A	N/A	0	N/A
<i>SAK/Plk4</i> CRISPR/OE	centriole/centrosome	N/A	N/A	0	1
<i>Sas-6</i> CRISPR/OE	PCM	N/A	N/A	0%–0.1%	0.4–1
<i>Slmb</i> CRISPR/allele	SCF complex/cell cycle	N/A	N/A	0%–0.3%	0.2–1
<i>tefu/ATM</i> RNAi/allele	serine/threonine kinase	N/A	N/A	0	1
Negative controls of genes that did not show differential expression in the female germline					
CG3436 allele	cell cycle	N/A	N/A	0	1

(Continued on next page)

Table 1. Continued

Variant	Function	Log ₂ fold change	P _{adj}	Total offspring (%)	p value
<i>dhd</i> allele	embryonic development	N/A	N/A	0	1
<i>Klp64D</i> RNAi/allele	motor protein	N/A	N/A	*	0.6–1
<i>Trx-2</i> RNAi/allele	redox	N/A	N/A	*	0.08–1
w RNAi/allele	eye pigment transporter	N/A	N/A	*	0.06–1

Summary of [Data S6A](#). Gene function was assigned from <https://flybase.org/>. The variants included knockdown lines (RNAi), mutant alleles (allele), genomic deficiencies including the indicated gene, CRISPR knockout alleles (CRISPR), and/or overexpression (OE) constructs. The log₂ fold change in transcript level and the p_{adj} value are given only for the comparison of expression differences between parthenogenetic and sexually reproducing *D. mercatorum* strains. Parthenogen offspring produced were calculated relative to the number of virgin females screened. Results marked with an asterisk (*) are considered false positives with no instances of facultative parthenogenesis indicated as “0.” All p values were calculated using Fisher’s exact test. See also [Figure S3](#) and [Data S2, S3, S5, and S6A](#).

genes that were either not differentially expressed or not expressed at all in mature *D. mercatorum* eggs ([Table 1](#)). For each gene tested, we used multiple independently created gene variants, when available ([Data S6A](#)).

Together, we screened 44 candidate genes and 5 control genes, of which 16 were able to produce between 0.1% and 0.4% parthenogenetic offspring per female in *D. melanogaster* when their expression was either increased or decreased ([Table 1](#); [Data S6A](#)). Although we observed parthenogenetic development from late embryonic to adult stages, parthenogenetic offspring most frequently died before hatching following such manipulation of a single gene. We also observed facultative parthenogenesis following manipulation of control genes, suggesting that stochastic facultative parthenogenesis is not just a feature of wild-caught *D. melanogaster*²⁰ ([Data S4B](#)) but also of lab stocks.

The low level of facultative parthenogenesis led us to re-screen the 16 identified genes in different pairwise combinations. This double gene variant screen eliminated all but 5 genes, which, in specific combinations, enabled sexually isolated females to generate between 0.5% and 11.4% offspring that also died between late embryonic stages and adulthood ([Figure 3A](#); [Data S6B](#)). We were unable to increase the frequency of facultative parthenogenesis further by genetically manipulating three or more gene variants (data not shown). All combinations resulting in increased facultative parthenogenesis included two extra copies of *polo* as a functional GFP-tagged transgene on the X chromosome and an allele of *Desat2*, which encodes an enzyme that desaturates double bonds in various hydrocarbons.^{41–44} Combination of *GFP-polo*⁺ with a mutant allele of *slmb*, which encodes a component of the Skp, Cullin, and F-box (SCF) ubiquitin-protein ligase, led to 3.1% facultative parthenogenesis ([Figure 3A](#)). Combination of *GFP-polo*⁺ with an allele of *Desat1*, which has 85% amino-acid identity with *Desat2*, gave up to 5.2% facultative parthenogenesis ([Figure 3A](#)). Finally, combination of *GFP-polo*⁺ with a duplication of *Myc* translocated onto the third chromosome showed 11.4% facultative parthenogenesis ([Figure 3A](#)). The *Desat2* allele is a known natural variant present in most populations⁴⁴; it was present in all *Desat1*, *Myc*, *GFP-polo*, and *slmb* stocks and could potentially cause the background of stochastic facultative parthenogenesis present in natural populations of *D. melanogaster* ([Data S6A](#)).²⁰ The TM6B “balancer” chromosome, which carries several inversions to prevent recombination and the dominant markers *Humeral* and *Tubby*,⁴⁵ does not carry the *Desat2* allele

and was used to balance the *Desat1*, *Desat2*, *Myc*, and *slmb* alleles.

Having identified gene expression changes in *D. mercatorum* that can induce facultative parthenogenesis when replicated in *D. melanogaster*, we searched for differences in organization of these genes between sexually reproducing and parthenogenetic *D. mercatorum* strains. Expression of *Desat2* is decreased by almost 100-fold in parthenogenetic *D. mercatorum* eggs in the absence of substantive changes in gene organization ([Figure S4A](#)). However, we cannot exclude the possibility of changes to distal enhancer elements or epigenetic differences between strains that could affect transcription factor binding. We also observed significant expression changes in transcription factor genes that could lie upstream of this and other differentially expressed genes ([Data S3A–S3D](#)). Neither *Desat1*, *polo*, nor *slmb* was differentially expressed nor did they have any substantive changes associated with their loci ([Figures S4B–S4D](#)). This was expected since we had tested *Desat1* as a functional counterpart of *Desat2* and *polo* as a substitute for the heightened expression of many centrosome/centriole genes. We tested *slmb* as part of the SCF ubiquitin-protein ligase responsible for both the degradation of *Myc* and *Plk4*; loss of *slmb* function thus leads to elevated *Myc* and *Plk4*. Moreover, in many tissues, both *polo* and *slmb* are under the control of *Myc*, raising the possibility of their differential expression at other developmental stages. The only differentially expressed gene identified by our screen having extensive genomic changes with the potential for effects on transcription, translation, or protein stability in the parthenogenetic *D. mercatorum* was *Myc* ([Figure S4E](#)). As *Myc* is known to broadly influence the expression of genes involved in cell growth, size, metabolism, apoptosis, and autophagy in *D. melanogaster*,⁴⁶ future work will be required to distinguish the effect of the individual changes to the *Myc* locus on these processes.

The proportion of facultative parthenogenetic offspring reaching adulthood from *GFP-polo*⁺;*Myc*^{dp} *Desat2*⁻/TM6B females was 1.4% ([Figure 3A](#); [Data S6B](#)). We created stable sexually reproducing *D. melanogaster* lines for each of the three combinations of variants showing the greatest level of facultative parthenogenesis, *GFP-polo*⁺;*Desat2*⁻/TM6B], *GFP-polo*⁺;*Desat2*⁻ *Desat1*⁻/TM6B], and *GFP-polo*⁺;*Myc*^{dp} *Desat2*⁻/TM6B]. We observed 0.1% adult offspring from *GFP-polo*⁺;*Desat2*⁻/TM6B] females, 0.2% adult offspring from *GFP-polo*⁺;*Desat2*⁻ *Desat1*⁻/TM6B] females, and 0.7% adult offspring from *GFP-polo*⁺;*Myc*^{dp} *Desat2*⁻/TM6B] females ([Figure 3B](#)). This is within the range of facultative parthenogenesis achieved

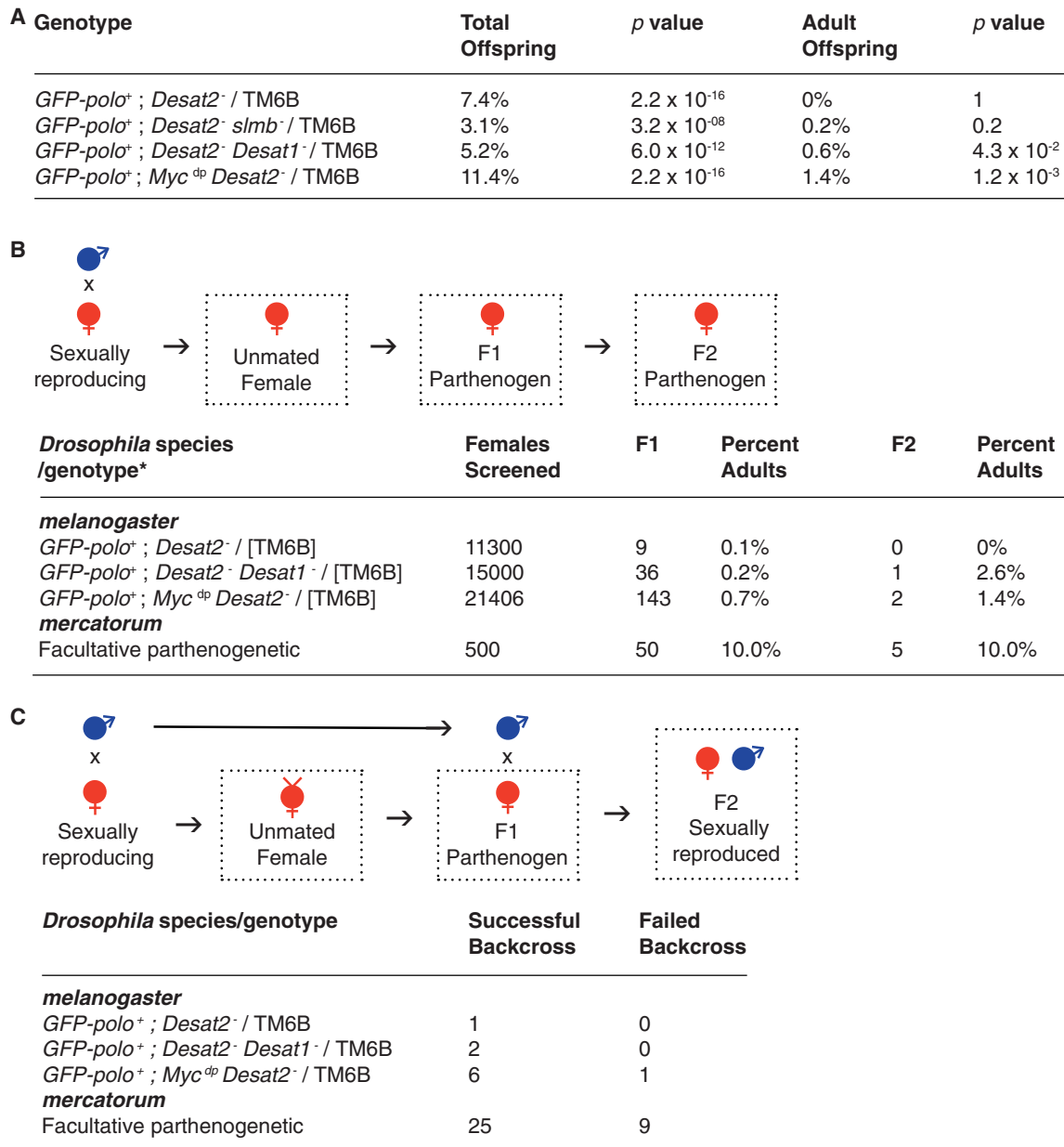


Figure 3. Facultative parthenogenesis and reproductive potential in *Drosophila*

(A) Double gene variant combinations resulting in facultative parthenogenesis in *D. melanogaster*. Summary of Data S6B. Only significantly facultative parthenogenetic combinations are shown. It is important to note that the genotype is heterozygous for the alleles indicated; all but *slmb*⁻ are homozygous viable (Data S6B). *p* value was calculated using the Fisher's exact test.

(B) The three gene variant combinations leading to significant development in induced facultative parthenogenetic *D. melanogaster* and facultative parthenogenetic *D. mercatorum* were screened for a second generation of parthenogenesis. TM6B is shown in parentheses because the balancer was not always present as the alleles it was balancing were homozygous viable.

(C) Parthenogenetically produced offspring from the induced facultative parthenogenetic *D. melanogaster* lines or produced naturally from the facultative parthenogenetic *D. mercatorum* were backcrossed to the parental line to determine if they could produce progeny in the F2 generation. *GFP-polo*⁺ is a transgene on the X, *Desat2*⁻ is a 5' UTR deletion, *Desat1*⁻ is a TE insertion, *Myc*^{dp} is a gene duplication on the 3rd chromosome, and *slmb*⁻ is a null allele.

See also Figure S4 and Data S6B.

by sexually reproducing *D. mercatorum* strains (0%–10.7%; Data S1B). Moreover, we found that both the *GFP-polo*⁺; *Desat2*⁻ *Desat1*⁻/ [TM6B] and *GFP-polo*⁺; *Myc*^{dp} *Desat2*⁻/ [TM6B] parthenogen females were able to parthenogenetically produce second-generation adult flies, as also found with

facultatively parthenogenetic *D. mercatorum* (Figure 3B). The *D. melanogaster* parthenogen offspring also retained the ability to mate with males from the parental sexually reproducing population to produce fertile progeny, as also found in facultatively parthenogenetic *D. mercatorum* (Figure 3C). Therefore,

both the genetically induced facultative parthenogenetic *D. melanogaster* and naturally facultatively parthenogenetic *D. mercatorum* offspring can reproduce both parthenogenetically and sexually. The genetic changes facilitating facultative parthenogenesis can be transmitted through generations, regardless of whether they undertake sexual or parthenogenetic reproduction.

Facultative parthenogenetic embryo development

To gain insight into parthenogenesis, we followed the development of facultative parthenogenetic embryos from completion of female meiosis onward. The drosophilid egg retains all four haploid meiotic products, three polar body nuclei and the female pronucleus, and if fertilized, the haploid male pronucleus. In both fertilized and unfertilized eggs, the three polar bodies migrate to the egg cortex where they may or may not fuse to form an arrested rosette-like configuration that we term a polar body aggregate; the mechanisms of aggregate formation and its migration are unknown. In the great majority of fertilized eggs, the polar body aggregate persists throughout syncytial development. However, in unfertilized eggs, polar body nuclei may enter mitosis where they become arrested.⁴⁷ Facultatively parthenogenetic *D. mercatorum* females produced eggs that either only formed polar body aggregates and stopped developing (Figure 4A), that entered the first mitosis and stopped developing (Figure 4B), or that entered multiple mitotic cycles of embryonic development (Figure 4C). We found that 12% of the *D. mercatorum* facultative parthenogenetic eggs undertook multiple nuclear division cycles in comparison with 38% of fully parthenogenetic eggs, whereas 15%–17% of both strains initiated the first mitosis and stopped developing. Some 71% of unfertilized eggs from facultatively parthenogenetic females and 48% from obligate parthenogenetic females remained arrested after polar body aggregate formation (Figures 4A–4D and S5B). By contrast, all *D. mercatorum* embryos generated through sexual reproduction undertook multiple rounds of nuclear division (Figures 4D and S5A). Unfertilized parthenogenetic and facultative parthenogenetic embryos developed with abnormal numbers of nuclei (Figure 4C) showing abnormalities in anaphase chromatid segregation (Figure S5B) in accordance with previous descriptions.^{36,37}

Fertilized *D. melanogaster* eggs behaved similarly to their *D. mercatorum* counterparts in initiating multiple cycles of mitotic divisions (Figures 4E and S5C). Without fertilization, 25% of the wild-type *D. melanogaster* eggs had a polar body aggregate, and 75% appeared to have entered the first mitotic nuclear division, but none completed it (Figures 4E and S5D). Of the unfertilized eggs overexpressing *polo*, having the *Desat2* allele, or having the *Myc* duplication and the *Desat2* allele, between 48% and 60% had polar body aggregates and 40% and 55% initiated the first mitosis suggestive of a state intermediate between fertilized and unfertilized wild-type eggs (Figure 4F). Two groups of unfertilized eggs undertook multiple division cycles: 6% of eggs overexpressing *polo* and having the *Desat2* allele (Figures 4F and 4G) and 16% of eggs overexpressing *polo* and having the *Desat2* allele plus the *Myc* duplication (Figures 4F and 4H). Therefore, two extra copies of *polo* and one fewer of *Desat2* is sufficient to initiate development in 6% of embryos, an effect enhanced to 16% by addition of a single extra copy of *Myc*. The proportion of eggs having completed meiosis to form a polar body aggregate was significantly reduced in the presence of an extra copy of *Myc*,

demonstrating increased entry into mitosis in unfertilized eggs (Figures 4F and 4H). The proportion of embryos initiating induced facultative parthenogenesis in *D. melanogaster* embryos (16%) is comparable with that seen in wild-type facultatively parthenogenetic *D. mercatorum* embryos (12%). However, although 10.7% of facultative parthenogenetic *D. mercatorum* progeny developed to adulthood, only 1.4% of the engineered facultative parthenogenetic *D. melanogaster* progeny could do so. Thus, additional factors appear likely to facilitate development beyond the embryonic stage of *D. melanogaster* parthenogens. Indeed, our screen focused only upon differentially expressed genes at the initiation of parthenogenesis and not upon zygotic requirements for later development. In facultatively parthenogenetic *D. mercatorum*, evolutionary changes in zygotic gene expression could enable efficient completion of development. Such a mechanism could include tissue-dependent control of *Myc* overexpression, which is able to regulate cell proliferation in many tissues, but it is possible that additional zygotically active factors remain to be discovered. Facultatively parthenogenetic *D. melanogaster* embryos further resembled their parthenogenetic *D. mercatorum* counterparts in failing to show precise repeated doubling of nuclei in a geometric series and in displaying lagging anaphase chromosomes during nuclear division (Figures 4G and 4H). Although parthenogenetic embryos show such abnormalities, only a single nucleus is needed to divide repeatedly during early embryogenesis to generate viable offspring.

The above observations led us to monitor the presence or absence of polar bodies in relation to the extent of mitotic progression in all single and double gene variant *D. melanogaster* eggs (Figure 5A). Unfertilized eggs with elevated *Polo* displayed a shift in the number of nuclei entering mitosis compared with unfertilized wild-type eggs, suggesting an effect upon progression of the nuclear division cycles (Figures 5A–5C). The *Desat2*[−] allele not only caused an increased proportion of eggs entering mitosis, compared with *GFP-polo*⁺ eggs but also caused the polar body nuclei to be positioned interiorly and thus a decrease in the number of eggs with a polar body aggregate at the cortex (Figure 5A). The addition of the *Myc* duplication further decreased the number of eggs arrested in development after polar body aggregate formation and increased the number of embryos undertaking multiple nuclear divisions (Figure 5A). The combination of *polo* overexpression and *Desat2*[−] increased the proportion of embryos undergoing multiple mitotic cycles at the expense of embryos with internalized nuclei (Figures 5A and 5D), and this was enhanced by the addition of the *Myc* duplication to this combination (Figures 5A and 5E).

The presence of GFP-tagged *Polo* in combinations favoring progression of unfertilized embryos into mitotic cycles allowed us to follow the distribution of *Polo* kinase on the mitotic apparatus. Whenever polar body chromosomes remained in a condensed state, no GFP-*Polo* could be found in their vicinity (Figures 5B and S6). However, whenever polar body chromosomes entered mitosis, GFP-*Polo* was associated with multiple microtubule-organizing centers (MTOCs) in the vicinity of the mitotic apparatus (arrowheads, Figures 5C, 5D, and S6) reminiscent of the multiple centrosomes seen in the parthenogenetic eggs of other *Drosophila* species.^{37,48} In addition, GFP-*Polo* showed a punctate distribution on mitotic kinetochores in numbers consistent with haploid, diploid, triploid, and tetraploid

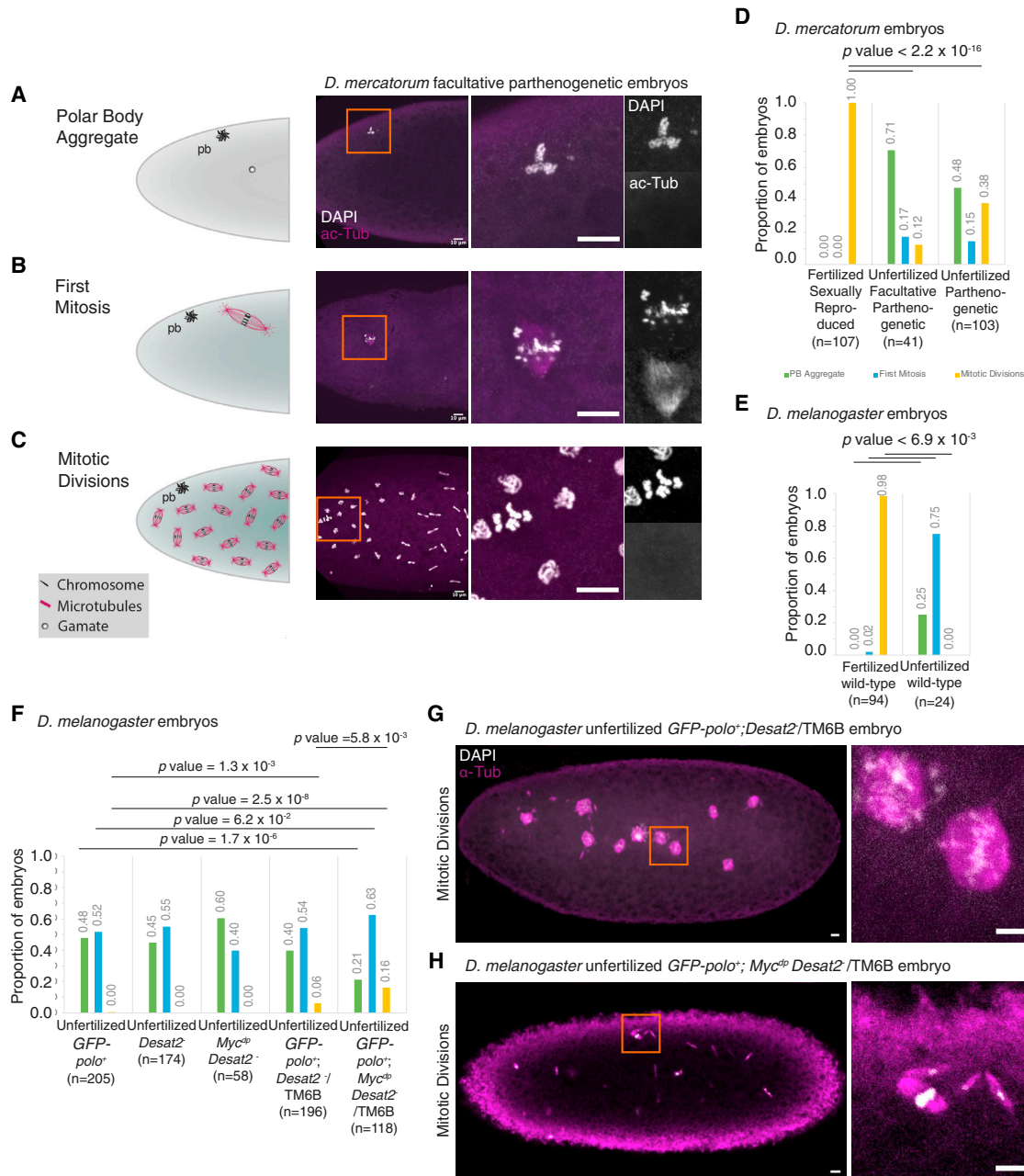


Figure 4. The inception of parthenogenesis *Drosophila* embryos

(A–C) Schematic showing the categorizations of development in embryos used in this study: formation of polar body (PB) aggregate, first mitosis, and subsequent mitotic divisions shown alongside examples of facultatively parthenogenetic *D. mercatorum* embryos of each category. DNA/DAPI (white) and acylated-Tubulin (ac-Tub) (magenta).

(D) Histogram displaying the proportion of fertilized, sexually reproduced, facultative parthenogenetic, and parthenogenetic *D. mercatorum* embryos that have completed meiosis and only have a PB aggregate present, initiated the first mitosis, or undertaken multiple mitotic nuclear divisions.

(E) Histogram displaying the proportion of wild-type fertilized and unfertilized *D. melanogaster* embryos that have completed meiosis and only have a PB aggregate present, initiated the first mitosis, or undertaken multiple mitotic nuclear divisions.

(F) Histogram displaying the proportion of unfertilized *D. melanogaster* eggs/embryos from *GFP-polo⁺*, *Desat2⁻*, *Myc^{dp} Desat2⁻*, *GFP-polo⁺; Desat2⁻/TM6B*, and *GFP-polo⁺; Myc^{dp} Desat2⁻/TM6B* mothers that have completed meiosis and only have a PB aggregate present, initiated the first mitosis, or undertaken multiple mitotic nuclear divisions.

(G and H) *D. melanogaster* embryos from *GFP-polo⁺; Desat2⁻/TM6B* and *GFP-polo⁺; Myc^{dp} Desat2⁻/TM6B* mothers that have undertaken multiple mitotic nuclear divisions. *GFP-polo⁺* is a transgene on the X, *Desat2⁻* is 5' UTR deletion, and *Myc^{dp}* is a locus duplication on the 3rd chromosome. DNA/DAPI (white) and α -Tubulin (magenta). Scale bars, 10 μ m. Fisher's exact test used to calculate p values.

See also Figure S5.

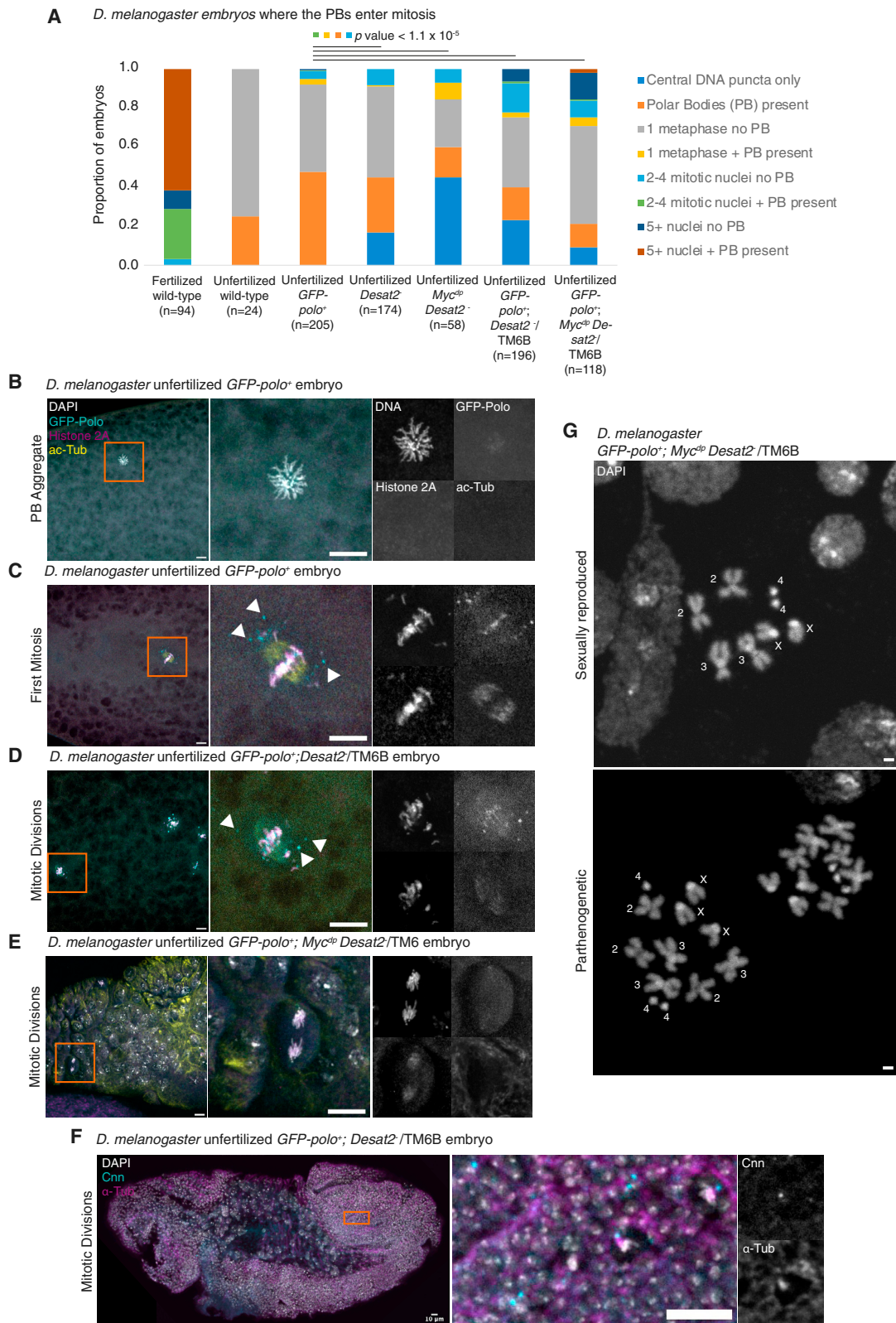


Figure 5. Initiation of parthenogenesis in genetically modified *D. melanogaster* embryos

(A) Stacked column chart showing the proportion of embryos that had a central DNA puncta, polar body (PB) aggregate, 1 single metaphase nuclei, 1 single metaphase nuclei and PB aggregate, 2–4 mitotic nuclei, 2–4 mitotic nuclei and PB aggregate, 5 or more mitotic nuclei, and 5 or more mitotic nuclei and PB

(legend continued on next page)

complements of chromosomes (Figures 5C, 5D, and S6). Thus, elevated Polo kinase appears to enable polar body aggregates to progress through mitosis in the presence of the *Desat2*⁻ allele, and this is enhanced by increased gene dosage of *Myc*. As the animals develop further, centrosomal GFP-Polo puncta are found only at the ends of the mitotic spindle as part of the MTOCs (Figure 5E). By the end of embryogenesis, mitotic centrosomes recruit Centrosomin (Cnn), part of the peri-centriolar material enabling centrosomes to recruit gamma-tubulin and nucleate a high density of spindle microtubules, demonstrating centrosome functionality in the parthenogenetic *D. melanogaster* embryos (Figure 5F). The formation of MTOCs, which develop into centrosomes is thus similar to that observed in other *Drosophila* species.^{37,48,49}

The above observations pointed toward the development of parthenogenetic offspring of various ploidies. In natural development, one of the four meiotic products becomes separated from the other three, giving the possibility of generating either haploid or triploid nuclei, the latter through either fusion of nuclei or their incorporation onto a common mitotic spindle. Similarly, two haploid nuclei may enter a common mitosis to generate a diploid product. We speculated that triploid nuclei might arise frequently in parthenogenetic offspring because this is a commonly found arrangement of polar body chromosomes in the wild-type embryo. This led us to examine the karyotype of offspring in cells best suited for this purpose, neuroblasts from third instar larval brains. This revealed that 6 of 12 (50%) parthenogenetically generated individuals examined were indeed triploid (Figure 5G). One individual was tetraploid, possibly representing fusion between all three polar body nuclei and the pronucleus. The remaining 5 (42%) were diploid, representing the fusion of two products of meiosis. Thus, engineered *D. melanogaster* parthenogens appear to follow the pattern described for other parthenogenetic drosophilids, which undertake normal meiosis and then rediploidize their genomes by either fusion of haploid meiotic products or post-meiotic duplication of the haploid gamete.^{20,22,36,47,50–52} This is in accordance with previous findings that polyploidy is more common in parthenogenetic than sexually reproducing insects.⁵³ Polyploidy often arises through fertilization of an unreduced egg of a female undergoing parthenogenesis to generate a triploid lineage comprising two maternal and a single paternal genome copy.⁵³ Here, we provide an alternative mechanism for polyploidy in parthenogenetic animals, through fusion of more than two haploid post-meiotic nuclei in an unfertilized egg.

DISCUSSION

Our study identifies genes associated with facultative parthenogenesis in the fruit fly, *D. mercatorum*, that are able to impart this ability to a non-parthenogenetic fruit fly, *D. melanogaster*. Although a genetic basis for parthenogenesis has been previously inferred through trait selection and by genetically mapping parthenogenetic loci, this is the first demonstration of genetically inducible facultative parthenogenesis in any animal. Together with physical and developmental constraints,² an identifiable genetic cause can account for the more frequent incidence of facultative parthenogenesis in particular groups of animals. The system we have developed to assess the contribution of gene variants to facultative parthenogenesis in *D. melanogaster* may be more broadly applicable to further parthenogenetic species of *Drosophila* and other forms of parthenogenesis. Moreover, our genetically induced strain of *D. melanogaster* provides a valuable tool for future mechanistic studies of parthenogenesis.

We demonstrate that two extra copies of *polo* coupled with decreased *Desat2* expression is sufficient to initiate embryogenesis in unfertilized *D. melanogaster* eggs and that this is enhanced by an extra copy of *Myc*. Progression through the nuclear division cycles of the syncytial embryo is very sensitive to the gene dosage of *polo* particularly when the cell cycle is under perturbation. For example, developmental failure of embryos from hemizygous *polo* mothers with hyperactive mitotic protein kinase, Greatwall, which inhibits PP2A, can be rescued by a single extra copy of *polo*.⁵⁴ This requirement for a delicate balance of Polo may reflect differing roles of Polo kinase to counter PP2A in promoting mitotic entry and yet collaborate with PP2A at later mitotic stages. The transition between meiosis and entry into the very first division cycle also requires cooperation between PP2A and the PanGu protein kinase; the *png* mutant phenotype, endoreduplication of the meiotic products to form giant nuclei, is suppressed by loss of PP2A function.⁵⁵ Precise control of cell-cycle parameters is therefore crucial for successful initiation of embryonic development, and Polo has a well-established role in initiating mitosis. Furthermore, in addition to initiating the nuclear division cycles, Polo also mediates the formation of centrosomal MTOCs (Figures 5C–5E) that, although not necessary for mitosis at later developmental stages,⁵⁶ are required for the rapid nuclear division cycles of the syncytial embryo.⁵⁷

aggregate from fertilized and unfertilized wild-type *D. melanogaster* embryos and embryos from *GFP-polo*⁺, *Desat2*⁻, *Myc^{dp} Desat2*⁻, *GFP-polo*⁺; *Desat2*⁻/TM6B, and *GFP-polo*⁺; *Myc^{dp} Desat2*⁻/TM6B mothers. Fisher's exact test used to calculate p values for all categories that had PB aggregates.

(B) PB aggregate in an unfertilized embryo from a *GFP-polo*⁺ mother.

(C) PB aggregate in an unfertilized embryo that initiated mitosis from a *GFP-polo*⁺ mother.

(D) A nucleus in mitosis in an embryo from a *GFP-polo*⁺; *Desat2*⁻/TM6B mother. Arrowheads point to ectopic centrosomes. When mitosis is initiated multiple GFP-Polo puncta form, and GFP-Polo becomes associated with the DNA and mitotic spindle in the PB aggregates that initiate mitosis and nuclei that continue mitosis alike.

(E) Nuclei in an embryo, from a *GFP-polo*⁺; *Myc^{dp} Desat2*⁻/TM6B mother, that has passed the cellularization stage of development. DNA/DAPI (white), GFP-Polo (cyan), Histone 2A (magenta), and acetylated-Tubulin (ac-Tub) (yellow).

(F) Cellularized embryo, from a *GFP-polo*⁺; *Desat2*⁻/TM6B mother, at extended germ-band stage. DNA/DAPI (white), centrosomes/cnn (cyan), and α -Tubulin (magenta).

(G) Mitotic karyotype chromosomes of third instar larval neuroblasts from sexually reproducing and parthenogenic *GFP-polo*⁺; *Myc^{dp} Desat2*⁻/TM6B *D. melanogaster* mothers. Neuroblasts in animals derived by sexual reproduction were all diploid ($n = 12$), whereas 50% of the parthenogenetically derived animals were triploid and 8%, tetraploid ($n = 12$). Individual chromosomes are labeled in white lettering.

Scale bars, 10 μ m (A–F) and 1 μ m (G). *GFP-polo*⁺ is a transgene on the X, *Desat2*⁻ is 5' UTR deletion, and *Myc^{dp}* is a locus duplication on the 3rd chromosome. See also Figure S6.

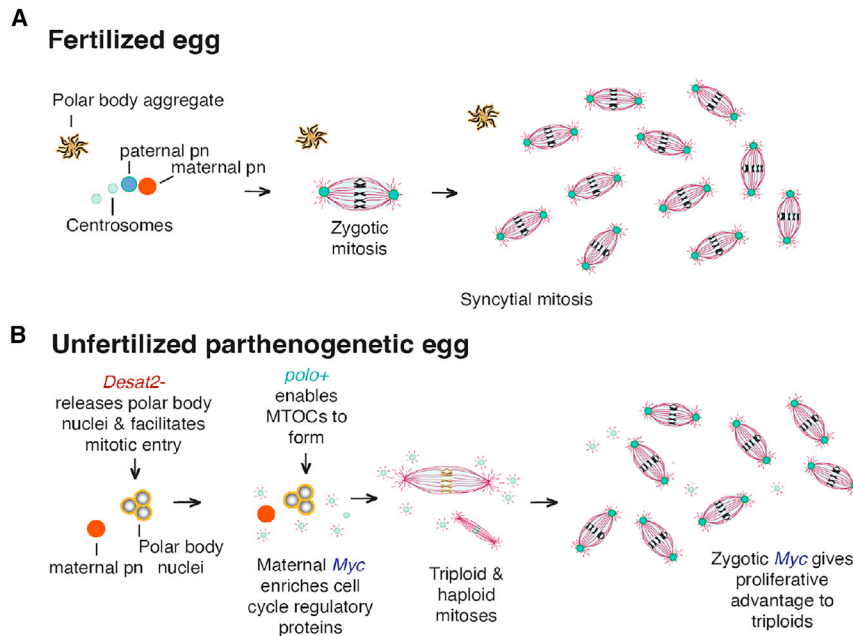


Figure 6. Proposed model for how *Myc*, *Polo*, and *Desat2* cause parthenogenesis in *D. melanogaster*

(A) In a fertilized egg the paternal pronucleus (pn) from the sperm and the maternal pn fuse and initiate cell divisions that are organized by centrosomes organized around a centriole and pro-centriole-like body provided by the sperm.

(B) Unfertilized eggs having greater maternal *Myc* expression exhibit increased expression of genes for cell-cycle regulatory proteins. The polar bodies (PBs) become positioned away from the egg membrane and can enter mitosis more readily as a result of the *Desat2*⁻ allele. Elevated Polo kinase promotes the *de novo* formation of centrosomes and facilitates entry into the mitotic cycles. As a consequence, the PB nuclei are exposed to all the components necessary to initiate development and the syncytial nuclear division cycles, thus initiating parthenogenesis. Once zygotic transcription is initiated, the elevated expression of *Myc* promotes cell proliferation favoring diploid or polyploid cells.

The greatest extent of development achieved in the single variant screen was with the *Desat1* allele, which also carried a background *Desat2*⁻ allele (Table 1; Data S6A). Decreased desaturase permitted the generation of adult flies parthenogenetically, which was not possible by increased *polo* or *Myc* expression alone. Decreased *Desat2* may have multifactorial consequences in initiating parthenogenetic development. *Desat2* influences the fluidity of membranes,^{41,44,58} which could interfere with the anchoring of polar body nuclei to the egg cortex, enabling them to adopt an interior position that is more favorable for mitosis and occurs in many parthenogen embryos carrying the *Desat2* allele (Figures 4G and 4H). *Desat2* is also present at the endoplasmic reticulum, whose integrity around the spindle poles is crucial to maintain mitotic spindle shape and pulling forces in the syncytial *Drosophila* embryo⁵⁹ that might be key for the onset of the mitotic division cycles. Moreover, the reticulated membrane surrounding the centrosome in *C. elegans* embryos also regulates both the microtubule nucleating ability of centrosomes and nuclear envelope breakdown on mitotic entry.⁶⁰ Continuity of the ER and nuclear membranes may be critical, not only for mitosis but also for the onset of zygotic development where the nuclear envelope forms *de novo*. In *D. melanogaster*, the egg-to-embryo transition requires the maternally provided YA nuclear membrane protein to initiate the syncytial mitotic cycles.⁶¹ Embryos derived from *fs(1)Ya* mothers lack this nuclear envelope protein and are unable to initiate the syncytial mitotic cycles. It is possible that membrane fluidity may play a role in mediating this transition together with specific nuclear envelope proteins.

Our identification of *Myc*, also known as *diminutive*, as an enhancer of facultative parthenogenesis is in line with its contribution to cell growth, cell competition, and regenerative proliferation. Its ability to promote cell proliferation in all tissues could give a necessary growth advantage to triploid or tetraploid cells in an otherwise genetically mosaic parthenogen facilitating development to adulthood. *Myc* plays an essential role in promoting

the rapid growth that must occur in both the germline and the surrounding follicle cells for oogenesis to proceed⁶² and is necessary to stimulate mitochondrial respiration in the ovary.⁶³ Thus, its elevated expression could be critical to express a wide range of genes to ensure that eggs are sufficiently fit for the proliferative challenges of parthenogenetic development.

Taken together, we propose a model for parthenogenetic development as a starting point for future research (Figure 6). Guided by differential gene expression between parthenogenetic and sexually reproducing strains of *D. mercatorum*, we identify three genes whose altered expression results in parthenogenesis in *D. melanogaster*. *Myc* is required for multiple aspects of the development of the *Drosophila* egg chamber and would ensure that the oocyte is optimally primed with gene products for the rapid nuclear division cycles of the syncytial embryo. Altered membrane fluidity resulting from decreased *Desat2* that would either release polar body nuclei from the egg membrane or prevent their transport to the membrane, thus facilitating their participation in mitosis to generate diploid, triploid, and tetraploid nuclei to populate the syncytium. Finally, increased Polo kinase would enable formation of multiple centrosomes in the parthenogenetic embryo upon the completion of meiosis. These are captured by the early mitotic figures ensuring the fidelity of subsequent mitoses but, perhaps more importantly, enabling the development of spatially organized MTOCs, essential to orchestrate the rapid nuclear division cycles. Following cellularization, elevated expression of *Myc* would ensure the growth and proliferation of tissues throughout all subsequent development.

Facultative parthenogenesis is potentially an adaptive trait that may provide reproductive assurance for isolated females.^{21,64–66} It is also possible that one or more of the variants we identified may have additional benefits in addition to reproductive assurance. In fact, decreased expression of the *Desat2* imparts cold tolerance to *D. melanogaster*, therefore aiding it to become a cosmopolitan species.⁴⁴ Thus, facultative parthenogenesis in

Drosophila may be under balancing selection together with other benefits. Facultative parthenogenesis appears to be a successful means of reproduction from its prevalence in *Drosophila*, midges, and mosquitos.² It seems likely therefore that facultative parthenogenesis in other dipteran species may share common underlying mechanisms that will be of considerable interest in the study of the control of insect populations.

STAR★METHODS

Detailed methods are provided in the online version of this paper and include the following:

- KEY RESOURCES TABLE
- RESOURCE AVAILABILITY
 - Lead contact
 - Materials Availability
 - Data and Code availability
- METHOD DETAILS
 - *Drosophila* stocks
 - *Drosophila* CRISPR
 - Hybridization experiments
 - Facultative Parthenogenesis assay
 - Wolbachia test
 - Selection of *D. mercatorum* strains to sequence
 - High molecular weight DNA preparation
 - Long-read Nanopore library preparation
 - Short-read Illumina library preparation
 - Genome assembly
 - Genome alignment
 - Genome coverage analysis
 - Self-heterozygosity and inter-strain divergence analysis
 - Mercury k-mer spectrum analysis
 - *De novo* genome annotation
 - Nucmer and gene distribution analysis
 - Genome assembly content
 - BUSCO analysis
 - Mitotic chromosome preparation
 - Polytene chromosome preparation
 - Molecular Instruments HCR sample preparation
 - RNA library preparation
 - Differential gene expression analysis
 - Gene Ontology (GO) analysis
 - *Drosophila* facultative parthenogenesis screen
 - *Desat2* allele screening
 - Second generation facultative parthenogenesis
 - Embryo preparation
 - Imaging
- QUANTIFICATION AND STATISTICAL ANALYSIS

ACKNOWLEDGMENTS

We would like to thank Isabel Palacios, John Welch, and Jose Casal for reading the manuscript and/or discussions about the work. We would like to thank Richard Durbin for advice, discussions, and computation assistance and Frank Jiggins for advice and discussions. We would like to thank Jonathan Day (Frank Jiggins's Lab) and Bettina Fischer (Richard Durbin's Lab) for advice on library preparation, technical assistance, protocols, reagents, and endless patience. We would like to thank Harry Choi and Mike Liu from Molecular

Instruments for troubleshooting and for gifted reagents during optimization of the HCR *in situ* protocol for use on DNA. We thank Pallavi Panda for a transgenic Rcd4 fly stock, Paula Almeida-Coelho for technical advice on *in situ* hybridization and karyotyping techniques, and Frank Sprenger for flies, kindly brought to Cambridge. We are grateful to the Genetics Fly Facility for embryo injections, particularly Dr. Alla Madich for multiple attempts to develop transgenics in *D. mercatorum*. We thank TRIP at Harvard Medical School (NIH/NIGMS R01-GM084947) for providing transgenic RNAi fly stocks used in this study. The genomics analysis was supported by NIH/NIDA U01DA047638 and NIH/NIGMS R01GM123489 (E.G.). The biological and gene expression work was supported by the Leverhulme Trust Project Grant (RPG-2018-229) and the Wellcome Trust Institutional Strategic Support Fund (RG89305) (D.M.G. and A.L.S.).

AUTHOR CONTRIBUTIONS

A.L.S. conceived this study, performed all biological experiments, and wrote the first draft of the manuscript. D.K.F. performed all gene expression related analysis and genome annotations. E.G. performed all genomics related analysis. A.L.S., D.K.F., E.G., and D.M.G. contributed to choices in methodology, experimental design, and the interpretation of results. Funding for the genomics analysis was obtained by E.G. The funding for all biological experiments, data, and gene expression analysis was obtained by A.L.S. and D.M.G.

DECLARATION OF INTERESTS

The authors declare no competing interests.

INCLUSION AND DIVERSITY

One or more of the authors of this paper self-identifies as an underrepresented ethnic minority in their field of research or within their geographical location. One or more of the authors of this paper self-identifies as a gender minority in their field of research. One or more of the authors of this paper self-identifies as living with a disability. While citing references scientifically relevant for this work, we also actively worked to promote gender balance in our reference list.

Received: April 17, 2023

Revised: June 4, 2023

Accepted: July 5, 2023

Published: July 28, 2023

REFERENCES

1. Suomalainen, E. (1950). Parthenogenesis in animals. *Adv. Genet.* 3, 193–253. [https://doi.org/10.1016/S0065-2660\(08\)60086-3](https://doi.org/10.1016/S0065-2660(08)60086-3).
2. Sperling, A.L., and Glover, D.M. (2023). Parthenogenesis in dipterans: a genetic perspective. *Proc. Biol. Sci.* 290, 20230261. <https://doi.org/10.1098/rspb.2023.0261>.
3. Surani, M.A.H., Barton, S.C., and Norris, M.L. (1984). Development of reconstituted mouse eggs suggests imprinting of the genome during gametogenesis. *Nature* 308, 548–550.
4. McGrath, J., and Solter, D. (1984). Completion of mouse embryogenesis requires both the maternal and paternal genomes. *Cell* 37, 179–183. [https://doi.org/10.1016/0092-8674\(84\)90313-1](https://doi.org/10.1016/0092-8674(84)90313-1).
5. Wei, Y., Yang, C.R., and Zhao, Z.A. (2022). Viable offspring derived from single unfertilized mammalian oocytes. *Proc. Natl. Acad. Sci. USA* 119, e2115248119. <https://doi.org/10.1073/pnas.2115248119>.
6. Braun, A.L., Meghini, F., Villa-Fombuena, G., Guermont, M., Fernandez-Martinez, E., Qian, Z., Dolores Martin-Bermudo, M., González-Reyes, A., Glover, D.M., and Kimata, Y. (2021). The careful control of Polo kinase by APC/C-Ube2C ensures the intercellular transport of germline centrosomes during *Drosophila* oogenesis. *Open Biol.* 11, 200371. <https://doi.org/10.1098/rsob.200371>.
7. Pimenta-Marques, A., Bento, I., Lopes, C.A.M., Duarte, P., Jana, S.C., and Bettencourt-Dias, M. (2016). A mechanism for the elimination of the female gamete centrosome in *Drosophila melanogaster*. *Science* 353, aaf4866.

8. Debec, A., Sullivan, W., and Bettencourt-Dias, M. (2010). Centrioles: active players or passengers during mitosis? *Cell. Mol. Life Sci.* 67, 2173–2194. <https://doi.org/10.1007/s00018-010-0323-9>.
9. Klotz, C., Dabauvalle, M.C., Paintrand, M., Weber, T., Bornens, M., and Karsenti, E. (1990). Parthenogenesis in *Xenopus* eggs requires centrosomal integrity. *J. Cell Biol.* 110, 405–415. <https://doi.org/10.1083/jcb.110.2.405>.
10. Wang, P., Yang, F., Ma, Z., and Zhang, R. (2021). Chromosome unipolar division and low expression of *Tws* may cause parthenogenesis of rice water Weevil (*Lissorhoptrus oryzophilus* Kuschel). *Insects* 12, <https://doi.org/10.3390/insects12040278>.
11. Xu, S., Huynh, T.V., and Snyman, M. (2022). The transcriptomic signature of obligate parthenogenesis. *Heredity* (Edinb) 128, 132–138. <https://doi.org/10.1038/s41437-022-00498-1>.
12. Lynch, M., Seyfert, A., Eads, B., and Williams, E. (2008). Localization of the genetic determinants of meiosis suppression in *Daphnia pulex*. *Genetics* 180, 317–327. <https://doi.org/10.1534/genetics.107.084657>.
13. Sandrock, C., and Vorburget, C. (2011). Single-locus recessive inheritance of asexual reproduction in a parasitoid wasp. *Curr. Biol.* 21, 433–437. <https://doi.org/10.1016/j.cub.2011.01.070>.
14. Yagound, B., Dogantzis, K.A., Zayed, A., Lim, J., Broekhuysse, P., Remnant, E.J., Beekman, M., Allsopp, M.H., Aamidor, S.E., Dim, O., et al. (2020). A single gene causes thelytokous parthenogenesis, the defining feature of the cape honeybee *Apis mellifera capensis*. *Curr. Biol.* 30, 2248–2259.e6. <https://doi.org/10.1016/j.cub.2020.04.033>.
15. Stelzer, C.P., Schmidt, J., Wiedroither, A., and Riss, S. (2010). Loss of sexual reproduction and dwarfing in a small metazoan. *PLoS One* 5, <https://doi.org/10.1371/journal.pone.0012854>.
16. Matsuda, M., and Tobari, Y.N. (2004). Genetic analyses of several *Drosophila ananassae*-complex species show a low-frequency major gene for parthenogenesis that maps to chromosome 2. *Genet. Res.* 83, 83–89. <https://doi.org/10.1017/s0016672303006657>.
17. Jaron, K.S., Bast, J., Nowell, R.W., Ranallo-Benavidez, T.R., Robinson-Rechavi, M., Schwander, T., and Orive, M. (2021). Genomic features of parthenogenetic animals. *J. Hered.* 112, 19–33. <https://doi.org/10.1093/jhered/esaa031>.
18. Olsen, M.W., Wilson, S.P., and Marks, H.L. (1968). Genetic control of parthenogenesis in chickens. *J. Hered.* 59, 41–42. <https://doi.org/10.1093/oxfordjournals.jhered.a107639>.
19. Nabours, R.K. (1919). Parthenogenesis and crossing-over in the grouse locust *Apotettix*. *Am. Nat.* 53, 131–142. <https://doi.org/10.1086/279700>.
20. Stalker, H.D. (1954). Parthenogenesis in *Drosophila*. *Genetics* 39, 4–34. <https://doi.org/10.1093/genetics/39.1.4>.
21. Carson, H.L. (1967). Selection for parthenogenesis in *Drosophila mercatorum*. *Genetics* 55, 157–171. <https://doi.org/10.1093/genetics/55.1.157>.
22. Carson, H.L., Wei, I.Y., and Niederkorn, J.A., Jr. (1969). Isogenicity in parthenogenetic strains of *Drosophila mercatorum*. *Genetics* 63, 619–628. <https://doi.org/10.1093/genetics/63.3.619>.
23. Carson, H.L., Teramoto, L.T., and Templeton, A.R. (1977). Behavioral differences among isogenic strains of *Drosophila mercatorum*. *Behav. Genet.* 7, 189–197. <https://doi.org/10.1007/BF01066275>.
24. Suvorov, A., Kim, B.Y., Wang, J., Armstrong, E.E., Peede, D., D'Agostino, E.R.R., Price, D.K., Waddell, P., Lang, M., Courtier-Orgogozo, V., et al. (2022). Widespread introgression across a phylogeny of 155 *Drosophila* genomes. *Curr. Biol.* 32, 111–123.e5. <https://doi.org/10.1016/j.cub.2021.10.052>.
25. O'Grady, P.M., and Markow, T.A. (2012). Chapter 18. Rapid morphological, behavioral, and ecological evolution in *Drosophila*: comparisons between the endemic Hawaiian *Drosophila* and the cactophilic *repleta* species group. In *Rapidly Evolving Genes and Genetic Systems*, First Edition (Oxford), pp. 176–186. <https://doi.org/10.1093/acprof:oso/9780199642274.003.0018>.
26. Templeton, A.R. (1979). The parthenogenetic capacities and genetic structures of sympatric populations of *Drosophila mercatorum* and *Drosophila hydei*. *Genetics* 92, 1283–1293. <https://doi.org/10.1093/genetics/92.4.1283>.
27. Muller, H.J. (1940). Bearings of the 'Drosophila' work on systematics. In *The New Systematics*, J.S. Huxley, ed. (Clarendon Press), pp. 185–268.
28. Sturtevant, A.H., and Novitski, E. (1941). The homologies of the chromosome elements in the genus *Drosophila*. *Genetics* 26, 517–541. <https://doi.org/10.1093/genetics/26.5.517>.
29. Schaeffer, S.W., Bhutkar, A., McAllister, B.F., Matsuda, M., Matzkin, L.M., O'Grady, P.M., Rohde, C., Valente, V.L., Aguadé, M., Anderson, W.W., et al. (2008). Polytene chromosomal maps of 11 *Drosophila* species: the order of genomic scaffolds inferred from genetic and physical maps. *Genetics* 179, 1601–1655. <https://doi.org/10.1534/genetics.107.086074>.
30. Wasserman, M. (1960). Cytological and phylogenetic relationships in the *repleta* group of the genus *Drosophila*. *Proc. Natl. Acad. Sci. USA* 46, 842–859. <https://doi.org/10.1073/pnas.46.6.842>.
31. Wasserman, M. (1963). Cytology and phylogeny of *Drosophila*. *Am. Nat.* 97, 333–352. <https://doi.org/10.1086/282284>.
32. Pritchett, T.L., Tanner, E.A., and McCall, K. (2009). Cracking open cell death in the *Drosophila* ovary. *Apoptosis* 14, 969–979. <https://doi.org/10.1007/s10495-009-0369-z>.
33. Avilés-Pagán, E.E., and Orr-Weaver, T.L. (2018). Activating embryonic development in *Drosophila*. *Semin. Cell Dev. Biol.* 84, 100–110. <https://doi.org/10.1016/j.semcdb.2018.02.019>.
34. Karsenti, E., Newport, J., Hubble, R., and Kirschner, M. (1984). Interconversion of metaphase and interphase microtubule arrays, as studied by the injection of centrosomes and nuclei into *Xenopus* eggs. *J. Cell Biol.* 98, 1730–1745. <https://doi.org/10.1083/jcb.98.5.1730>.
35. Maller, J., Poccia, D., Nishioka, D., Kidd, P., Gerhart, J., and Hartman, H. (1976). Spindle formation and cleavage in *Xenopus* eggs injected with centriole-containing fractions from sperm. *Exp. Cell Res.* 99, 285–294. [https://doi.org/10.1016/0014-4827\(76\)90585-1](https://doi.org/10.1016/0014-4827(76)90585-1).
36. Eisman, R.C., and Kaufman, T.C. (2007). Cytological investigation of the mechanism of parthenogenesis in *Drosophila mercatorum*. *Fly* 1, 317–329. <https://doi.org/10.4161/fly.5408>.
37. Riparbelli, M.G., and Callaini, G. (2003). *Drosophila* parthenogenesis: a model for de novo centrosome assembly. *Dev. Biol.* 260, 298–313. [https://doi.org/10.1016/S0012-1606\(03\)00243-4](https://doi.org/10.1016/S0012-1606(03)00243-4).
38. Rodrigues-Martins, A., Riparbelli, M., Callaini, G., Glover, D.M., and Bettencourt-Dias, M. (2007). Revisiting the role of the mother centriole in centriole biogenesis. *Science* 316, 1046–1050. <https://doi.org/10.1126/science.1142950>.
39. Wang, W.J., Soni, R.K., Uryu, K., and Bryan Tsou, M.F. (2011). The conversion of centrioles to centrosomes: essential coupling of duplication with segregation. *J. Cell Biol.* 193, 727–739. <https://doi.org/10.1083/jcb.201101109>.
40. Sunkel, C.E., and Glover, D.M. (1988). *polo*, a mitotic mutant of *Drosophila* displaying abnormal spindle poles. *J. Cell Sci.* 89, 25–38. <https://doi.org/10.1242/jcs.89.1.25>.
41. Dembeck, L.M., Böröczky, K., Huang, W., Schal, C., Anholt, R.R., and Mackay, T.F. (2015). Genetic architecture of natural variation in cuticular hydrocarbon composition in *Drosophila melanogaster*. *eLife* 4, e09861. <https://doi.org/10.7554/eLife.09861>.
42. Takahashi, A., Tsauro, S.C., Coyne, J.A., and Wu, C.I. (2001). The nucleotide changes governing cuticular hydrocarbon variation and their evolution in *Drosophila melanogaster*. *Proc. Natl. Acad. Sci. USA* 98, 3920–3925. <https://doi.org/10.1073/pnas.061465098>.
43. Dallerac, R., Labeur, C., Jallon, J.M., Knipple, D.C., Roelofs, W.L., and Wicker-Thomas, C. (2000). A delta 9 desaturase gene with a different substrate specificity is responsible for the cuticular diene hydrocarbon polymorphism in *Drosophila melanogaster*. *Proc. Natl. Acad. Sci. USA* 97, 9449–9454.
44. Greenberg, A.J., Moran, J.R., Coyne, J.A., and Wu, C.I. (2003). Ecological adaptation during incipient speciation revealed by precise gene replacement. *Science* 302, 1754–1757. <https://doi.org/10.1126/science.1090432>.

45. Miller, D.E., Cook, K.R., Arvanitakis, A.V., and Hawley, R.S. (2016). Third chromosome balancer inversions disrupt protein-coding genes and influence distal recombination events in *Drosophila melanogaster*. *G3 (Bethesda)* 6, 1959–1967. <https://doi.org/10.1534/g3.116.029330>.
46. Grifoni, D., and Bellosa, P. (2015). *Drosophila Myc*: a master regulator of cellular performance. *Biochim. Biophys. Acta* 1849, 570–581. <https://doi.org/10.1016/j.bbagr.2014.06.021>.
47. Doane, W.W. (1960). Completion of meiosis in unispermated eggs of *Drosophila melanogaster*. *Science* 132, 677–678. <https://doi.org/10.1126/science.132.3428.677>.
48. Hirai, K., Inoue, Y.H., and Matsuda, M. (2023). Mitotic progression and dual spindle formation caused by spindle association of de novo-formed microtubule-organizing centers in parthenogenetic embryos of *Drosophila ananassae*. *Genetics* 223, <https://doi.org/10.1093/genetics/iyac178>.
49. Riparbelli, M.G., and Callaini, G. (2008). *Drosophila* parthenogenesis: a tool to decipher centrosomal vs acentrosomal spindle assembly pathways. *Exp. Cell Res.* 314, 1617–1625. <https://doi.org/10.1016/j.yexcr.2008.01.030>.
50. Carson, H.L. (1973). The genetic system in parthenogenetic strains of *Drosophila mercatorum*. *Proc. Natl. Acad. Sci. USA* 70, 1772–1774. <https://doi.org/10.1073/pnas.70.6.1772>.
51. Chang, C.C., Ting, C.T., Chang, C.H., Fang, S., and Chang, H.Y. (2014). The persistence of facultative parthenogenesis in *Drosophila albomicans*. *PLoS One* 9, e113275. <https://doi.org/10.1371/journal.pone.0113275>.
52. Murdy, W.H., and Carson, H.L. (1959). Parthenogenesis in *Drosophila mangabeirai* Malog. *Am. Nat.* 93, 355–363. <https://doi.org/10.1086/282095>.
53. Otto, S.P., and Whitton, J. (2000). Polyploid incidence and evolution. *Annu. Rev. Genet.* 34, 401–437. <https://doi.org/10.1146/annurev.genet.34.1.401>.
54. Rangone, H., Wegel, E., Gatt, M.K., Yeung, E., Flowers, A., Debski, J., Dadlez, M., Janssens, V., Carpenter, A.T., and Glover, D.M. (2011). Suppression of scant identifies Endos as a substrate of greatwall kinase and a negative regulator of protein phosphatase 2A in mitosis. *PLoS Genet.* 7, e1002225. <https://doi.org/10.1371/journal.pgen.1002225>.
55. Lee, L.A., Elfring, L.K., Bosco, G., and Orr-Weaver, T.L. (2001). A genetic screen for suppressors and enhancers of the *Drosophila* PAN GU cell cycle kinase identifies cyclin B as a target. *Genetics* 158, 1545–1556. <https://doi.org/10.1093/genetics/158.4.1545>.
56. Basto, R., Lau, J., Vinogradova, T., Gardiol, A., Woods, C.G., Khodjakov, A., and Raff, J.W. (2006). Flies without centrioles. *Cell* 125, 1375–1386. <https://doi.org/10.1016/j.cell.2006.05.025>.
57. Rodrigues-Martins, A., Riparbelli, M., Callaini, G., Glover, D.M., and Bettencourt-Dias, M. (2008). From centriole biogenesis to cellular function: centrioles are essential for cell division at critical developmental stages. *Cell Cycle* 7, 11–16. <https://doi.org/10.4161/cc.7.1.5226>.
58. Sinclair, B.J., Gibbs, A.G., and Roberts, S.P. (2007). Gene transcription during exposure to, and recovery from, cold and desiccation stress in *Drosophila melanogaster*. *Insect Mol. Biol.* 16, 435–443. <https://doi.org/10.1111/j.1365-2583.2007.00739.x>.
59. Araújo, M., Tavares, A., Vieira, D.V., Telley, I.A., and Oliveira, R.A. (2023). Endoplasmic reticulum membranes are continuously required to maintain mitotic spindle size and forces. *Life Sci. Alliance* 6, 6. <https://doi.org/10.26508/lsa.202201540>.
60. Maheshwari, R., Rahman, M.M., Drey, S., Onyundo, M., Fabig, G., Martinez, M.A.Q., Matus, D.Q., Müller-Reichert, T., and Cohen-Fix, O. (2023). A membrane reticulum, the centriculum, affects centrosome size and function in *Caenorhabditis elegans*. *Curr. Biol.* 33, 791–806.e7. <https://doi.org/10.1016/j.cub.2022.12.059>.
61. Sackton, K.L., Lopez, J.M., Berman, C.L., and Wolfner, M.F. (2009). YA is needed for proper nuclear organization to transition between meiosis and mitosis in *Drosophila*. *BMC Dev. Biol.* 9, 43. <https://doi.org/10.1186/1471-213X-9-43>.
62. Maines, J.Z., Stevens, L.M., Tong, X., and Stein, D. (2004). *Drosophila* dMyc is required for ovary cell growth and endoreplication. *Development* 131, 775–786. <https://doi.org/10.1242/dev.00932>.
63. Wang, Z.H., Liu, Y., Chaitankar, V., Pirooznia, M., and Xu, H. (2019). Electron transport chain biogenesis activated by a JNK-insulin-Myc relay primes mitochondrial inheritance in *Drosophila*. *eLife* 8, e49309. <https://doi.org/10.7554/eLife.49309>.
64. Watts, P.C., Buley, K.R., Sanderson, S., Boardman, W., Ciofi, C., and Gibson, R. (2006). Parthenogenesis in Komodo dragons. *Nature* 444, 1021–1022. <https://doi.org/10.1038/4441021a>.
65. Burke, N.W., and Bonduriansky, R. (2017). Sexual conflict, facultative asexuality, and the true paradox of sex. *Trends Ecol. Evol.* 32, 646–652. <https://doi.org/10.1016/j.tree.2017.06.002>.
66. Booth, W., Smith, C.F., Eskridge, P.H., Hoss, S.K., Mendelson, J.R., 3rd, and Schuett, G.W. (2012). Facultative parthenogenesis discovered in wild vertebrates. *Biol. Lett.* 8, 983–985. <https://doi.org/10.1098/rsbl.2012.0666>.
67. Port, F., Chen, H.M., Lee, T., and Bullock, S.L. (2014). Optimized CRISPR/Cas tools for efficient germline and somatic genome engineering in *Drosophila*. *Proc. Natl. Acad. Sci. USA* 111, E2967–E2976. <https://doi.org/10.1073/pnas.1405500111>.
68. Ruan, J., and Li, H. (2020). Fast and accurate long-read assembly with wtdbg2. *Nat. Methods* 17, 155–158. <https://doi.org/10.1038/s41592-019-0669-3>.
69. Li, H. (2018). Minimap2: pairwise alignment for nucleotide sequences. *Bioinformatics* 34, 3094–3100. <https://doi.org/10.1093/bioinformatics/bty191>.
70. Li, H., Handsaker, B., Wysoker, A., Fennell, T., Ruan, J., Homer, N., Marth, G., Abecasis, G., and Durbin, R.; 1000 Genome Project Data Processing Subgroup (2009). The Sequence Alignment/Map format and SAMtools. *Bioinformatics* 25, 2078–2079. <https://doi.org/10.1093/bioinformatics/btp352>.
71. Garrison, E.K., and Marth, G. (2012). Haplotype-based variant detection from short-read sequencing. Preprint at arXiv. <https://doi.org/10.48550/arXiv.1207.3907>.
72. Li, H. (2011). A statistical framework for SNP calling, mutation discovery, association mapping and population genetical parameter estimation from sequencing data. *Bioinformatics* 27, 2987–2993. <https://doi.org/10.1093/bioinformatics/btr509>.
73. Guarracino, A., Mwaniki, N., Marco-Sola, S., and Garrison, E.K. (2021). wfmash: whole-chromosome pairwise alignment using the hierarchical wavefront algorithm. Version 0.7.0. (GitHub). <https://github.com/waveygang/wfmash/blob/master/CITATION.cff>.
74. Quinlan, A.R., and Hall, I.M. (2010). BEDTools: a flexible suite of utilities for comparing genomic features. *Bioinformatics* 26, 841–842. <https://doi.org/10.1093/bioinformatics/btq033>.
75. Rhie, A., Walenz, B.P., Koren, S., and Phillippy, A.M. (2020). Merqury: reference-free quality, completeness, and phasing assessment for genome assemblies. *Genome Biol.* 21, 245. <https://doi.org/10.1186/s13059-020-02134-9>.
76. Flynn, J.M., Hubley, R., Goubert, C., Rosen, J., Clark, A.G., Feschotte, C., and Smit, A.F. (2020). RepeatModeler2 for automated genomic discovery of transposable element families. *Proc. Natl. Acad. Sci. USA* 117, 9451–9457. <https://doi.org/10.1073/pnas.1921046117>.
77. Smit, A.F.A., Hubley, R., and Green, P. (1996–2010). RepeatMasker Open-3.0. <http://www.repeatmasker.org>.
78. Martin, M. (2011). Cutadapt removes adapter sequences from high-throughput sequencing reads. *EMBnet J.* 17, 10–12. <https://doi.org/10.14806/ej.17.1.200>.
79. Dobin, A., Davis, C.A., Schlesinger, F., Drenkow, J., Zaleski, C., Jha, S., Batut, P., Chaisson, M., and Gingeras, T.R. (2013). STAR: ultrafast universal RNA-seq aligner. *Bioinformatics* 29, 15–21. <https://doi.org/10.1093/bioinformatics/bts635>.

80. Brúna, T., Hoff, K.J., Lomsadze, A., Stanke, M., and Borodovsky, M. (2021). BRAKER2: automatic eukaryotic genome annotation with GeneMark-EP+ and AUGUSTUS supported by a protein database. NAR Genom. Bioinform. 3, lqaa108. <https://doi.org/10.1093/nargab/lqaa108>.
81. Zhang, Z., Schwartz, S., Wagner, L., and Miller, W. (2000). A greedy algorithm for aligning DNA sequences. J. Comput. Biol. 7, 203–214.
82. Kurtz, S., Phillippy, A., Delcher, A.L., Smoot, M., Shumway, M., Antonescu, C., and Salzberg, S.L. (2004). Versatile and open software for comparing large genomes. Genome Biol. 5, R12. <https://doi.org/10.1186/gb-2004-5-2-r12>.
83. Manni, M., Berkeley, M.R., Seppey, M., Simão, F.A., and Zdobnov, E.M. (2021). BUSCO update: novel and streamlined workflows along with broader and deeper phylogenetic coverage for scoring of eukaryotic, prokaryotic, and viral genomes. Mol. Biol. Evol. 38, 4647–4654. <https://doi.org/10.1093/molbev/msab199>.
84. Liao, Y., Smyth, G.K., and Shi, W. (2014). featureCounts: an efficient general purpose program for assigning sequence reads to genomic features. Bioinformatics 30, 923–930. <https://doi.org/10.1093/bioinformatics/btt656>.
85. Alexa, A., Rahnenführer, J., and Lengauer, T. (2006). Improved scoring of functional groups from gene expression data by decorrelating GO graph structure. Bioinformatics 22, 1600–1607. <https://doi.org/10.1093/bioinformatics/btl140>.
86. Schindelin, J., Arganda-Carreras, I., Frise, E., Kaynig, V., Longair, M., Pietzsch, T., Preibisch, S., Rueden, C., Saalfeld, S., Schmid, B., et al. (2012). Fiji: an open-source platform for biological-image analysis. Nat. Methods 9, 676–682. <https://doi.org/10.1038/nmeth.2019>.
87. Stouthamer, R., Breeuwer, J.A., Luck, R.F., and Werren, J.H. (1993). Molecular identification of microorganisms associated with parthenogenesis. Nature 361, 66–68. <https://doi.org/10.1038/361066a0>.
88. O'Neill, S.L., and Karr, T.L. (1990). Bidirectional incompatibility between conspecific populations of *Drosophila simulans*. Nature 348, 178–180. <https://doi.org/10.1038/348178a0>.
89. Stalker, H.D. (1964). The salivary gland chromosomes of *Drosophila nigro-melanica*. Genetics 49, 883–893. <https://doi.org/10.1093/genetics/49.5.883>.
90. Templeton, A.R., Carson, H.L., and Sing, C.F. (1976). The population genetics of parthenogenetic strains of *Drosophila mercatorum*. II The capacity for parthenogenesis in a natural, bisexual population. Genetics 82, 527–542. <https://doi.org/10.1093/genetics/82.3.527>.
91. Chen, H., Rangasamy, M., Tan, S.Y., Wang, H., and Siegfried, B.D. (2010). Evaluation of five methods for total DNA extraction from western corn root-worm beetles. PLoS One 5, e11963. <https://doi.org/10.1371/journal.pone.0011963>.
92. Miller, D.E., Staber, C., Zeitlinger, J., and Hawley, R.S. (2018). Highly contiguous genome assemblies of 15 *Drosophila* species generated using nanopore sequencing. G3 (Bethesda) 8, 3131–3141. <https://doi.org/10.1534/g3.118.200160>.
93. Sun, X., Wahlstrom, J., and Karpen, G. (1997). Molecular structure of a functional *Drosophila* centromere. Cell 91, 1007–1019. [https://doi.org/10.1016/S0092-8674\(00\)80491-2](https://doi.org/10.1016/S0092-8674(00)80491-2).
94. Biessmann, H., Valgeirsdottir, K., Lofsky, A., Chin, C., Ginther, B., Levis, R.W., and Pardue, M.L. (1992). HeT-A, a transposable element specifically involved in “healing” broken chromosome ends in *Drosophila melanogaster*. Mol. Cell. Biol. 2, 3910–3918.
95. Levis, R.W., Ganesan, R., Houtchens, K., Tolar, L.A., and Sheen, F.M. (1993). Transposons in place of telomeric repeats at a *Drosophila* telomere. Cell 75, 1083–1093.
96. Kaminker, J.S., Bergman, C.M., Kronmiller, B., Carlson, J., Svirskas, R., Patel, S., Frise, E., Wheeler, D.A., Lewis, S.E., Rubin, G.M., et al. (2002). The transposable elements of the *Drosophila melanogaster* euchromatin: a genomics perspective. Genome Biol. 3, RESEARCH0084.
97. Broderick, N.A., and Lemaitre, B. (2012). Gut-associated microbes of *Drosophila melanogaster*. Gut Microbes 3, 307–321. <https://doi.org/10.4161/gmic.19896>.
98. Brand, A.H., and Perrimon, N. (1993). Targeted gene expression as a means of altering cell fates and generating dominant phenotypes. Development 118, 401–415. <https://doi.org/10.1242/dev.118.2.401>.
99. Panda, P., Kovacs, L., Dzhindzhev, N., Fatalska, A., Persico, V., Geymonat, M., Riparbelli, M.G., Callaini, G., and Glover, D.M. (2020). Tissue specific requirement of *Drosophila* Rcd4 for centriole duplication and ciliogenesis. J. Cell Biol. 219, <https://doi.org/10.1083/jcb.201912154>.

STAR★METHODS

KEY RESOURCES TABLE

REAGENT or RESOURCE	SOURCE	IDENTIFIER
Antibodies		
Mouse α -acetylated-tubulin antibody, clone 6-11B-1 (1:200 dilution)	Merck/Sigma-Aldrich	MABT868; RRID:AB_2819178
Mouse α -tubulin antibody, DM1A (1:200 dilution)	Merck/Sigma-Aldrich	T6199; RRID:AB_477583
Rabbit α -Histone H2A antibody (1:500 dilution)	Abcam	ab13923; RRID:AB_300750
Rabbit α -cnn antibody (1:200 dilution)	Glover lab	N/A
Goat α -Mouse 488 (1:500 dilution)	Life Technologies (now ThermoFisher)	N/A
Goat α -Mouse 647 (1:500 dilution)	Life Technologies (now ThermoFisher)	N/A
Goat α -Rabbit 488 (1:500 dilution)	Invitrogen (now ThermoFisher)	A-11008; RRID:AB_143165
Goat α -Rabbit 647 (1:500 dilution)	Life Technologies (now ThermoFisher)	N/A
Chemicals, peptides, and recombinant proteins		
RNAlater Stabilization Solution	ThermoFisher	AM7020
Critical commercial assays		
Ligation Sequencing Kit	Nanopore	SQK LSK-109/ SQK LSK-110
Genomic-tip (100/G)	QIAGEN	Cat. No. / ID: 10243
KAPA HyperPrep Kits for NGS DNA Library Prep	Roche	Cat. No. / ID: KK8542
NEBNext Ultra II DNA Library Prep Kit	New England Biolabs	E7645S
RNAEasy kit	QIAGEN	Cat. No. / ID: 74104
KAPA mRNA HyperPrep Kit	Roche	N/A
Deposited data		
Transcriptomics data	This Paper	ENA: PRJEB43100
Genomics data	This Paper	ENA: PRJEB64421
Experimental models: Organisms/strains		
<i>D. melanogaster</i> P{ry[+t7.2]=neoFRT}19A; ry[506]	Bloomington Drosophila Stock Center	BDSC 1709
<i>D. melanogaster</i> w [*] ; P{w ^{+mW.hs} =FRT(w ^{hs})}2A	Bloomington Drosophila Stock Center	BDSC 1997
<i>D. melanogaster</i> w ¹¹¹⁸ ; Df(3R)ED5177, P{3'.RS5+3.3'}ED5177/TM6C, cu1 Sb1	Bloomington Drosophila Stock Center	BDSC 8103
<i>D. melanogaster</i> px1 bw1 mr1 sp1/ln(2LR)bwV1, ds33k bwV1	Bloomington Drosophila Stock Center	BDSC 380
<i>D. melanogaster</i> chl1 l(2)bw1 bw2b mr2/SM5	Bloomington Drosophila Stock Center	BDSC 257
<i>D. melanogaster</i> w[1118]; Df(3L)BSC418/TM6C, Sb[1] cu[1]	Bloomington Drosophila Stock Center	BDSC 24922
<i>D. melanogaster</i> w[1118]; Df(3L)BSC837/TM6C, Sb[1] cu[1]	Bloomington Drosophila Stock Center	BDSC 27916
<i>D. melanogaster</i> w[1118]; Df(3R)BSC794, P+PBac{w[+mC]=XP3.WH3}BSC794/TM6C, Sb[1] cu[1]]	Bloomington Drosophila Stock Center	BDSC 27366
<i>D. melanogaster</i> w[1118]; Df(3R)BSC508/TM6C, Sb[1] cu[1]	Bloomington Drosophila Stock Center	BDSC 27916
<i>D. melanogaster</i> pUbg-ana2 / CyO	Glover Lab	N/A
<i>D. melanogaster</i> UASp-Asl-WT/CyO	Glover Lab	N/A
<i>D. melanogaster</i> w; UASp-SAK/CyO; MKRS/TM6B	Glover Lab	N/A
<i>D. melanogaster</i> Ub-plp::GFP5.2/CyO; TM3, sb/TM6B	Ruslan Lab	N/A
<i>D. melanogaster</i> Sas-6 rescue pUbg-Sas-6 / CyO	Glover Lab	N/A
<i>D. melanogaster</i> y ¹ sc ¹ v ¹ P{nos-phiC31\int.NLS}X; P{CaryP}attP2	Bloomington Drosophila Stock Center	BDSC 25710

(Continued on next page)

Continued

REAGENT or RESOURCE	SOURCE	IDENTIFIER
<i>D. melanogaster</i> $y^1 v^1 P\{nos-\phi C31\int int.NLS\}X$; $P\{CaryP\}attP40$	Bloomington Drosophila Stock Center	BDSC 25709
<i>D. melanogaster nanos-cas9</i>	Filip Port	N/A
<i>D. melanogaster actin-cas9</i>	Filip Port	N/A
<i>D. mercatorum</i> wildtype	Cornell Stock Centre	CSC 15082-1511.00
<i>D. mercatorum</i> wildtype	Cornell Stock Centre	CSC 15082-1521.22
<i>D. mercatorum</i> wildtype	Cornell Stock Centre	CSC 15082-1527.01
<i>D. mercatorum</i> wildtype	Cornell Stock Centre	CSC 15082-1527.02
<i>D. mercatorum</i> wildtype	Cornell Stock Centre	CSC 15082-1527.03
<i>D. mercatorum</i> wildtype	Cornell Stock Centre	CSC 15082-1527.04
<i>D. mercatorum</i> wildtype	Cornell Stock Centre	CSC 15082-1527.05
<i>D. mercatorum</i> parthenogenetic	Cornell Stock Centre	CSC 15082-1525.07
<i>D. ananasea</i> wildtype	Cornell Stock Centre	CSC 14024-0371.15
<i>D. ananasea</i> wildtype	Francis Jiggins Lab	N/A
<i>D. atripex</i> wildtype	Cornell Stock Centre	CSC 14024-0361.00
<i>D. pallidosa</i> wildtype	Kyorin Fly	k-aae002
<i>D. suzukii</i> wildtype	Genetics Fly Facility	N/A
<i>D. parthenogenetica</i> wildtype	Cornell Stock Centre	CSC 15181-2221.03
<i>D. robusta</i> wildtype	Cornell Stock Centre	CSC 15020-1111.12
<i>D. albomicans</i> wildtype	Kyorin Fly	E-10801
<i>D. americana</i> wildtype	Cornell Stock Centre	CSC 15010-1041.32
<i>D. hydie</i> wildtype	Francis Jiggins Lab	N/A
<i>S. lebanonensis</i> wildtype	Francis Jiggins Lab	N/A
<i>S. stonei</i> wildtype	Francis Jiggins Lab	N/A
w <i>D. melanogaster</i> -	Genetics Fly Facility	N/A
<i>D. melanogaster</i> Or	Genetics Fly Facility	N/A
<i>D. melanogaster</i> wild-caught isofemale line - Single female collected in Cambridge UK, CB1 1DS	This study	N/A
<i>D. melanogaster</i> $y[1] w[*] P\{w[+mC]=bam-GAL4:VP16\}1$	Bloomington Drosophila Stock Center	BDSC 80579
<i>D. melanogaster</i> $w[*]; P\{w[+mC]=matalpha4-GAL-VP16\}V37$	Bloomington Drosophila Stock Center	BDSC 7063
<i>D. melanogaster</i> $w[*]; P\{w[+mC]=matalpha4-GAL-VP16\}V2H$	Bloomington Drosophila Stock Center	BDSC 7062
<i>D. melanogaster</i> $y[1] v[1]; P\{y[+t7.7] v[+t1.8]=TRiP.HMC02386\}attP2$	Bloomington Drosophila Stock Center	BDSC 44484
<i>D. melanogaster</i> $lf / CyO; MKRS / TM6B$	David M Glover Lab	N/A
<i>D. melanogaster</i> $y[1] w[*]; P\{y[+t7.7]=Mae-UAS.6.11\}CG3436[LA00324]$	Bloomington Drosophila Stock Center	BDSC 22228
<i>D. melanogaster</i> $dhd[JS] / FM7;; TM6B / TM3$	Terry Orr-Weaver Lab	N/A
<i>D. melanogaster</i> $dhd[P8] / FM7$	Terry Orr-Weaver Lab	N/A
<i>D. melanogaster</i> $y[1] v[1]; P\{y[+t7.7] v[+t1.8]=TRiP.HMS02193\}attP40$	Bloomington Drosophila Stock Center	BDSC 40945
<i>D. melanogaster</i> $y[1] w[1]; Klp64D[k1]/TM3, y[+] Ser[1]$	Bloomington Drosophila Stock Center	BDSC 5578
<i>D. melanogaster</i> $y[1] sc[*] v[1] sev[21]; P\{y[+t7.7] v[+t1.8]=TRiP.HMS00989\}attP2$	Bloomington Drosophila Stock Center	BDSC 34019
<i>D. melanogaster</i> $y[1] sc[*] v[1] sev[21]; P\{y[+t7.7] v[+t1.8]=TRiP.HMS00603\}attP2$	Bloomington Drosophila Stock Center	BDSC 33721
<i>D. melanogaster</i> [1118]; $P\{w[+mGT]=GT1\} Trx-2[BG02804]$	Bloomington Drosophila Stock Center	BDSC 12826

(Continued on next page)

Continued

REAGENT or RESOURCE	SOURCE	IDENTIFIER
<i>D. melanogaster</i> y[1] v[1]; P{y[+7.7] v[+1.8]=TRiP.HMS00017}attP2	Bloomington Drosophila Stock Center	BDSC 33623
<i>D. melanogaster</i> y[1] sc[*] v[1] sev[21]; P{y[+7.7] v[+1.8]=TRiP.GL00094}attP2	Bloomington Drosophila Stock Center	BDSC 35573
<i>D. melanogaster</i> y[1] v[1]; P{y[+7.7] v[+1.8]=TRiP.HMS00004}attP2/TM3, Sb[1]	Bloomington Drosophila Stock Center	BDSC 33613
<i>D. melanogaster</i> y[1] v[1]; P{y[+7.7] v[+1.8]=TRiP.HMJ21116}attP40/CyO	Bloomington Drosophila Stock Center	BDSC 51002
<i>D. melanogaster</i> y[1] v[1]; P{y[+7.7] v[+1.8]=TRiP.HMS00029}attP2	Bloomington Drosophila Stock Center	BDSC 33631
<i>D. melanogaster</i> Bam-gal4	Felipe Karam Teixeira Lab	N/A
<i>D. melanogaster</i> w[1118]; P{w[+mC]=osk-GAL4::VP16}A11/CyO	Bloomington Drosophila Stock Center	BDSC 44241
<i>D. melanogaster</i> w[1118]; P{y[+7.7] w[+mC]=GMR83E05-GAL4}attP2	Bloomington Drosophila Stock Center	BDSC 40361
<i>D. melanogaster</i> y[1] w[*]; P{w[+mC]=Act5C-GAL4}17bFO1/TM6B, Tb[1]	Bloomington Drosophila Stock Center	BDSC 3954
<i>D. melanogaster</i> ry[506] e[1] bam[Delta86]/TM3, ry[RK] Sb[1] Ser[1]	Bloomington Drosophila Stock Center	BDSC 5427
<i>D. melanogaster</i> y[1] v[1]; P{y[+7.7] v[+1.8]=TRiP.HMC04150}attP2	Bloomington Drosophila Stock Center	BDSC 55877
<i>D. melanogaster</i> w[*]; Df(3R)caki[X-313], CASK[X-313]/TM6B, Tb[+]	Bloomington Drosophila Stock Center	BDSC 6784
<i>D. melanogaster</i> y[1] v[1]; P{y[+7.7] v[+1.8]=TRiP.HMJ21478}attP40	Bloomington Drosophila Stock Center	BDSC 54035
<i>D. melanogaster</i> y[1] v[1]; P{y[+7.7] v[+1.8]=TRiP.HMC03034}attP2	Bloomington Drosophila Stock Center	BDSC 51428
<i>D. melanogaster</i> y[1] sc[*] v[1] sev[21]; P{y[+7.7] v[+1.8]=TRiP.HMC04435}attP40	Bloomington Drosophila Stock Center	BDSC 56993
<i>D. melanogaster</i> w[1118]; PBac{w[+mC]=WH}CG17202[f01979]/TM6B, Tb[1]	Bloomington Drosophila Stock Center	BDSC 18498
<i>D. melanogaster</i> y[1] sc[*] v[1] sev[21]; P{y[+7.7] v[+1.8]=TRiP.HMS02472}attP40	Bloomington Drosophila Stock Center	BDSC 42636
<i>D. melanogaster</i> y[1] sc[*] v[1] sev[21]; P{y[+7.7] v[+1.8]=TRiP.GL01585}attP2	Bloomington Drosophila Stock Center	BDSC 43975
<i>D. melanogaster</i> y[1] sc[*] v[1] sev[21]; P{y[+7.7] v[+1.8]=TRiP.HMC03583}attP40	Bloomington Drosophila Stock Center	BDSC 53354
<i>D. melanogaster</i> w[*]; b[1]; CRMP[<i>supK1</i>]	Bloomington Drosophila Stock Center	BDSC 40954
<i>D. melanogaster</i> y[1] sc[*] v[1] sev[21]; P{y[+7.7] v[+1.8]=TRiP.GL00428}attP2	Bloomington Drosophila Stock Center	BDSC 35591
<i>D. melanogaster</i> y[1] sc[*] v[1] sev[21]; P{y[+7.7] v[+1.8]=TRiP.HMS01654}attP40	Bloomington Drosophila Stock Center	BDSC 37512
<i>D. melanogaster</i> y[1] w[67c23]; P{y[+mDint2] w[+mC]=EPgy2}Desat1[EY07679]	Bloomington Drosophila Stock Center	BDSC 20171
<i>D. melanogaster</i> w[1118]; Df(3R)Exel7316/TM6B, Tb[1]	Bloomington Drosophila Stock Center	BDSC 7970
<i>D. melanogaster</i> y[1] v[1]; P{y[+7.7] v[+1.8]=TRiP.HMJ30095}attP40	Bloomington Drosophila Stock Center	BDSC 63529
<i>D. melanogaster</i> y[1] sc[*] v[1] sev[21]; P{y[+7.7] v[+1.8]=TRiP.HMC06291}attP2	Bloomington Drosophila Stock Center	BDSC 65995
<i>D. melanogaster</i> In(3L)P, Desat2[7-11HD-low]	Bloomington Drosophila Stock Center	BDSC 4532
<i>D. melanogaster</i> w[*] P{w[+mC]=EP}e(r)[G926]	Bloomington Drosophila Stock Center	BDSC 33462
<i>D. melanogaster</i> w[1118]; P{w[+mC]=UAS-eya.B.II}14	Bloomington Drosophila Stock Center	BDSC 5675

(Continued on next page)

Continued

REAGENT or RESOURCE	SOURCE	IDENTIFIER
<i>D. melanogaster</i> w[1118]; P{w[+mC]=UAS-eya.B.l}55.2	Bloomington Drosophila Stock Center	BDSC 5676
<i>D. melanogaster</i> y[1] sc[*] v[1] sev[21]; P{y[+t7.7] v[+t1.8]=TRiP.HMS02251}attP2	Bloomington Drosophila Stock Center	BDSC 41687
<i>D. melanogaster</i> f[36a]	Bloomington Drosophila Stock Center	BDSC 43
<i>D. melanogaster</i> y[1] sc[*] v[1] sev[21]; P{y[+t7.7] v[+t1.8]=TRiP.HMS00249}attP2	Bloomington Drosophila Stock Center	BDSC 33375
<i>D. melanogaster</i> w[*]; P{w[+mC]=lacW}FER [X42]/TM6B, Tb[1]	Bloomington Drosophila Stock Center	BDSC 9361
<i>D. melanogaster</i> y[1] w[*]; P{w[+mC]=UAS-gnu-GFP.R}2/CyO	Bloomington Drosophila Stock Center	BDSC 38438
<i>D. melanogaster</i> gnu[1] / TM6B	This study	N/A
<i>D. melanogaster</i> y[1] sc[*] v[1] sev[21]; P{y[+t7.7] v[+t1.8]=TRiP.HMC04660}attP40	Bloomington Drosophila Stock Center	BDSC 57266
<i>D. melanogaster</i> w[1118]; Tl{w[+mW.hs]=Tl}ktub[1]/CyO	Bloomington Drosophila Stock Center	BDSC 68206
<i>D. melanogaster</i> y[1] w[67c23]; P{y[+mDint2] w[+mC]=EPgy2}msd1[EY11673]	Bloomington Drosophila Stock Center	BDSC 20814
<i>D. melanogaster</i> Myc[4]/FM7i, P{w[+mC]=ActGFP}JMR3	Bloomington Drosophila Stock Center	BDSC 64769
<i>D. melanogaster</i> w[1118]; Dp(1;3)DC059, PBac{y[+mDint2] w[+mC]=DC059}VK00033	Bloomington Drosophila Stock Center	BDSC 31438
<i>D. melanogaster</i> w[1118]; Dp(1;3)DC060, PBac{y[+mDint2] w[+mC]=DC060}VK00033/TM6C, Sb[1]	Bloomington Drosophila Stock Center	BDSC 30239
<i>D. melanogaster</i> w[1118]; P{w[+mC]=UAS-Myc.Z}132	Bloomington Drosophila Stock Center	BDSC 9674
<i>D. melanogaster</i> y[1] w[*]; P{w[+mC]=UAS-Nmnat.Z}2/CyO	Bloomington Drosophila Stock Center	BDSC 39699
<i>D. melanogaster</i> w[1118]; P{w[+mC] pnt[P2.UAS]=UAS-pnt.P2}2/TM3, Sb[1]	Bloomington Drosophila Stock Center	BDSC 399
<i>D. melanogaster</i> w[*]; Rack1[1.8] P{ry[+t7.2]=neoFRT}40A/CyO, S[2]	Bloomington Drosophila Stock Center	BDSC 24152
<i>D. melanogaster</i> pUAS-GFP-Rcd4 / SM5a	David M Glover lab	N/A
<i>D. melanogaster</i> pUAS-flag-Rcd4 / SM5a	David M Glover lab	N/A
<i>D. melanogaster</i> pUbq-GFP-Rcd4	David M Glover lab	N/A
<i>D. melanogaster</i> pUbq-Rcd4-GFP	David M Glover lab	N/A
<i>D. melanogaster</i> w[*]; P{w[+mC]=UAS-Roc1a.D}8.1	Bloomington Drosophila Stock Center	BDSC 34047
<i>D. melanogaster</i> Roc1A[4] / FM6B	This study	N/A
<i>D. melanogaster</i> w[*] P{w[+mC]=EP}Roc1a[G824]/FM6, w[*]	Bloomington Drosophila Stock Center	BDSC 26607
<i>D. melanogaster</i> y[1]; P{y[+mDint2] w[BR.E.BR]=SUPor-P}RpL10Ab[KG09231] ry[506]/TM3, Sb[1] Ser[1]	Bloomington Drosophila Stock Center	BDSC 15173
<i>D. melanogaster</i> w[*]; P{w[+mC]=UASsp-spir.RC.GFP}21	Bloomington Drosophila Stock Center	BDSC 24765
<i>D. melanogaster</i> ana2[4.3] / CyO	This study	N/A
<i>D. melanogaster</i> pUbq-Asl-wt / CyO	David M Glover lab	N/A
<i>D. melanogaster</i> asl[FL.Ubi-p63E.EYFP]	Cayetano Gonzalez Lab	N/A
<i>D. melanogaster</i> asl[38] / TM6B	This study	N/A
<i>D. melanogaster</i> cn[1] cnn[HK21] bw[1]/CyO, l(2)DTS513[1]	Bloomington Drosophila Stock Center	BDSC 5039

(Continued on next page)

Continued

REAGENT or RESOURCE	SOURCE	IDENTIFIER
<i>D. melanogaster</i> w[*]; P{w[+mC]=UAS-CycE.L}ML1	Bloomington Drosophila Stock Center	BDSC 4781
<i>D. melanogaster</i> y[1]; P{y[+mDint2]w[BR.E.BR]=SUPor-P}Exo70[KG08051] mtrm[KG08051] ry[506]/TM3, Sb[1] Ser[1]	Bloomington Drosophila Stock Center	BDSC 14932
<i>D. melanogaster</i> mr[1] / CyO	This study	N/A
<i>D. melanogaster</i> mr[2] / CyO	This study	N/A
<i>D. melanogaster</i> plp[165-P3-16] / TM6B	This study	N/A
<i>D. melanogaster</i> plu[1] / CyO	This study	N/A
<i>D. melanogaster</i> plu[5] / CyO	This study	N/A
<i>D. melanogaster</i> png[14] / FM7	This study	N/A
<i>D. melanogaster</i> png[1] / FM7	This study	N/A
<i>D. melanogaster</i> P{GFP-polo[+]} endogenous promotor	Claudio Sunkel Lab	N/A
<i>D. melanogaster</i> w[1118]; Dp(3;2)GV-CH321-86F01, PBac{y[+mDint2] w[+mC]=GV-CH321-86F01}VK00037/CyO	Bloomington Drosophila Stock Center	BDSC 90053
<i>D. melanogaster</i> polo[1] / TM6B	David M Glover lab	N/A
<i>D. melanogaster</i> polo[11] / TM3	David M Glover lab	N/A
<i>D. melanogaster</i> UAS-rca1; if / CyO; MKRS / TM6B	Frank Sprenger Lab	N/A
<i>D. melanogaster</i> UAS-rca1 / CyO; MKRS / TM6B	Frank Sprenger Lab	N/A
<i>D. melanogaster</i> w; pUASp-SAK / CyO; MKRS, Sb / TM6B	David M Glover lab	N/A
<i>D. melanogaster</i> w[1118]; Dp(3;2)GV-CH321-48C20, PBac{y[+mDint2] w[+mC]=GV-CH321-48C20}VK00037/CyO	Bloomington Drosophila Stock Center	BDSC 90163
<i>D. melanogaster</i> SAK[144] / TM6B	This study	N/A
<i>D. melanogaster</i> pUbp-Sas-6-GFP / CyO	David M Glover lab	N/A
<i>D. melanogaster</i> If / Cyo; pUASp-Sas6 GFP / TM6B	David M Glover lab	N/A
<i>D. melanogaster</i> Sas-6[103] / TM6B	This study	N/A
<i>D. melanogaster</i> w[*]; P{ry[+7.2]=neoFRT}82B slmb[3A1]/TM6B, Tb[+]	Bloomington Drosophila Stock Center	BDSC 65423
<i>D. melanogaster</i> w[*]; P{ry[+7.2]=neoFRT}82B slmb[UU11]/TM6B, Tb[1]	Bloomington Drosophila Stock Center	BDSC 65424
<i>D. melanogaster</i> w[1118]; Df(3R)BSC508/TM6C, Sb[1] cu[1]	Bloomington Drosophila Stock Center	BDSC 25012
<i>D. melanogaster</i> slmb[i33] / TM6B	This study	N/A
<i>D. melanogaster</i> slmb[i41] / TM6B	This study	N/A
<i>D. melanogaster</i> slmb[i44] / TM6B	This study	N/A
<i>D. melanogaster</i> y[1] sc[*] v[1] sev[21]; P{y[+7.7] v[+1.8]=TRiP.HMS02790}attP40	Bloomington Drosophila Stock Center	BDSC 44073
<i>D. melanogaster</i> y[1] sc[*] v[1] sev[21]; P{y[+7.7] v[+1.8]=TRiP.GL00138}attP2	Bloomington Drosophila Stock Center	BDSC 44417
<i>D. melanogaster</i> w[*]; P{ry[+7.2]=neoFRT}82B tefu[atm-6] e[1]/TM6B, Tb[1]	Bloomington Drosophila Stock Center	BDSC 8626
<i>D. melanogaster</i> P{ry[+7.2]=neoFRT}82B tefu[atm-8] e[1]/TM3, Sb[1]	Bloomington Drosophila Stock Center	BDSC 8624
Oligonucleotides		
Wolbachia TGGTCCAATAAGTGATGAAGAAAC	Julien Martinez	wsp 81F

(Continued on next page)

Continued

REAGENT or RESOURCE	SOURCE	IDENTIFIER
Wolbachia AAAAATTAACGCTACTCCA	Julien Martinez	wsp 691R
<i>Desat2</i> AAGAGCTCGCCAGCTATCTAC	This study	<i>Desat2</i> -UTR-FWD
<i>Desat2</i> AAGGACACCCGTTTCTCTGG	This Study	<i>Desat2</i> -UTR-REV
Recombinant DNA		
Plasmid CFD4	Port et al. ⁶⁷	CFD4
Software and algorithms		
CRISPR Optimal Target Finder	N/A	http://tools.flycrispr.molbio.wisc.edu/targetFinder/)
wtdbg2 (v2.5)	Ruan and Li ⁶⁸	https://github.com/ruanjue/wtdbg2
minimap2 (v2.24)	Li ⁶⁹	https://github.com/lh3/minimap2/releases
Samtools	Li et al. ⁷⁰	https://www.htslib.org/
Freebayes	Garrison and Marth ⁷¹	https://github.com/freebayes/freebayes
bcftools consensus (v2.18)	Li ⁷²	https://github.com/samtools/bcftools/releases/
wfmash (v0.6)	Guarracino et al. ⁷³	https://github.com/waveygang/wfmash/releases
bedtools (v2.18)	Quinlan and Hall ⁷⁴	https://github.com/arq5x/bedtools2
meryl (v1.3) and) and merqury (v1)	Rhie et al. ⁷⁵	https://github.com/marbl/meryl
RepeatModeler2 (v2.0.1)	Flynn et al. ⁷⁶	https://github.com/Dfam-consortium/RepeatModeler/blob/master/RELEASE-NOTES
RepeatMasker (v4.0.9)	Smit et al. ⁷⁷	https://www.repeatmasker.org/
cutadapt (v2.0)	Martin ⁷⁸	https://cutadapt.readthedocs.io/en/v2.0/
STAR (v2.7.0e)	Dobin et al. ⁷⁹	https://github.com/alexdobin/STAR/releases
BRAKER2	Brüna et al. ⁸⁰	https://github.com/Gaius-Augustus/BRAKER
BLASTx (ncbi-blast-2.10.1)	Zhang et al. ⁸¹	https://ftp.ncbi.nlm.nih.gov/blast/documents/blastdb.html
MUMmer (v3.23)	Kurtz et al. ⁸²	https://mummer.sourceforge.net/
BUSCO (v5.3.2)	Manni et al. ⁸³	https://busco.ezlab.org/
featureCounts (subread v1.6.3)	Liao et al. ⁸⁴	https://rnsh.github.io/bioinfo-notebook/docs/featureCounts.html
topGO	Alexa et al. ⁸⁵	https://bioconductor.org/packages/release/bioc/html/topGO.html
ImageJ (Fiji)	Schindelin et al. ⁸⁶	https://fiji.sc/
Other		
R9 Version Spot-ON Flow Cell RevD	Nanopore	FLO-MIN106D
Molecular Instruments HCR protocol (v3.0)	Molecular Instruments	https://www.molecularinstruments.com/hcr-rnafish-protocols
<i>D. melanogaster</i> gene names and FBgn numbers	http://flybase.org/	fbgn_NAseq_Uniprot_fb_2020_03.tsv
<i>D. melanogaster</i> CDS (reference version 6.35) and Genome (v6.27)	N/A	https://www.ncbi.nlm.nih.gov/genome?term=vih&cmd=DetailsSearch
<i>D. melanogaster</i> Genome Release 6 plus ISO1 MT	The FlyBase Consortium/Berkeley Drosophila Genome Project/Celera Genomics	https://www.ncbi.nlm.nih.gov/assembly/GCF_000001215.4/

RESOURCE AVAILABILITY

Lead contact

Further information and requests for resources and reagents should be directed to and will be fulfilled by the lead contact, Alexis Sperling (alb84@cam.ac.uk).

Materials Availability

All *Drosophila* stocks generated in the study will be made available upon request.

Data and Code availability

- All code is publicly available. The genome assembly, analysis, and quality control code are on <https://github.com/ekg/Drosophila>. The annotation, transcriptomics analysis, and quality control code are on https://github.com/FabianDK/drosophila_parthenogenesis
- All raw and analyzed *D. mercatorum* genomic data is available on ENA (European Nucleotide Archive): PRJEB64421.
- The gene expression data generated by this study is on ENA: PRJEB43100.
- Any additional information required to reanalyze the data reported in this paper is available from the lead contact upon request.

METHOD DETAILS

Drosophila stocks

All screened alleles have their origin and stock numbers also given in the appropriate data tables to the facilitate matching of results with alleles (Data S1, S4, and S6). The stocks used in creating CRISPR/Cas9-generated alleles, complementation test, and rescue experiments are listed below:

FRT chromosome stock $P\{ry[+t7.2]=neoFRT\}19A$; $ry[506]$ (BDSC 1709). FRT chromosome stock w^* ; $P\{w^{+mW.hs}=FRT(w^{hs})\}2A$ (BDSC 1997). *asl* deficiency w^{1118} ; $Df(3R)ED5177$, $P\{3'.RS5+3.3'\}ED5177/TM6C$, $cu1$ $Sb1$ (BDSC 8103). *morula* mutant alleles $px1$ $bw1$ $mr1$ $sp1/In(2LR)bwV1$, $ds33k$ $bwV1$ (BDSC 380) and $chl1$ $l(2)bw1$ $bw2b$ $mr2/SM5$ (BDSC 257). *Plk4/SAK* deficiency $w[1118]$; $Df(3L)BSC418/TM6C$, $Sb[1]$ $cu[1]$ (BDSC 24922). *plp* deficiency $w[1118]$; $Df(3L)BSC837/TM6C$, $Sb[1]$ $cu[1]$ (BDSC 27916). *Sas-6* deficiency $w[1118]$; $Df(3R)BSC794$, $P+PBac\{w[+mC]=XP3.WH3\}BSC794/TM6C$, $Sb[1]$ $cu[1]$ (BDSC 27366). *slmb* deficiency $w[1118]$; $Df(3R)BSC508/TM6C$, $Sb[1]$ $cu[1]$ (BDSC 27916). *ana2* rescue $pUbq-ana2$ / *CyO* (Glover Lab). *asl* rescue: *UASp-Asl-WT/CyO* (Glover Lab). *Plk4/SAK* rescue w ; *UASp-SAK/CyO*; *MKRS/TM6B* (Glover Lab). *plp* rescue *Ub-plp::GFP5.2/CyO*; *TM3*, *sb/TM6B* (Ruslan Lab). *Sas-6* rescue *pUbq-Sas-6* / *CyO* (Glover Lab).

Drosophila CRISPR

The CRISPR/Cas9 stocks were created using *nos-cas9* and *act-cas9* from Phillip Port crossed with a transgenic line expressing the gRNA using the exact method and flies described previously.^{6,67} The CRISPR Optimal Target Finder (<http://tools.flycrispr.molbio.wisc.edu/targetFinder/>) was used to design the 20mer target sequence. Transgenic gRNA flies were created with either y^1 sc^1 v^1 $P\{nos-phiC31\}int.NLS\}X$; $P\{CaryP\}attP2$ (BDSC 25710) or y^1 v^1 $P\{nos-phiC31\}int.NLS\}X$; $P\{CaryP\}attP40$ (BDSC 25709). The gRNA sequences (Data S5) were cloned into plasmid CFD4⁶⁷ and injected into embryos by the Genetics Fly Facility, University of Cambridge, thereby creating transgenic gRNA-expressing stocks. To screen for successful mutations the genomic DNA was isolated, a PCR was run with primers to the gene in question (Data S5) and Sanger sequenced.

Hybridization experiments

The reciprocal crosses of males and females from different *D. mercatorum* strains were maintained for the duration of their lives with their food changed weekly. If offspring (F1) were produced, they were checked for the presence of at least 3 males, since *D. mercatorum* does produce non-disjunction males (X/0) by parthenogenesis.²¹ The F1 were then flipped into a new tube and checked for male and female offspring (F2). If F2 were produced, then both the males and the females were fertile. All strains of *D. mercatorum* were able to interbreed producing viable and fertile male and female offspring, although the parthenogenetically reproducing strain showed some impediment in consistent sexual reproduction (Data S1A).

Facultative Parthenogenesis assay

The facultative parthenogenesis assay was adapted from Stalker 1954.²⁰ Batches of 1-70 virgins were collected and maintained for the duration of their lives on fresh food that was changed weekly. All offspring screening was carried out blind. The old food was kept for more than 3 days and then examined for parthenogenetic development, indicated by the presence of dead brown embryos (dead embryos turn brown if they have tissues decaying) or further development. Any observed offspring was allowed to reach its final stage of development. If a fly was parthenogenetically produced, it was then maintained for the duration of its life on fresh food. We documented the number of instances of facultative parthenogenesis relative to the number of adults screened. Our determination of the

baseline of facultative parthenogenesis in 8 different *D. mercatorum* strains indicated that most offspring were produced midway through the mother's life (22.2 days out of the average 50 days; [Data S1B](#)).

Wolbachia test

Parthenogenesis did not arise as a result of Wolbachia infections as is known to occur in other arthropods⁸⁷ because we confirmed by PCR that the *D. mercatorum* strains did not carry Wolbachia ([Data S1B](#)). Moreover, in *Drosophila* Wolbachia infections are only reported to cause cytoplasmic incompatibility.⁸⁸ Together, these findings validate the use of *D. mercatorum* as our study species; the strains to be used for comparison; and of the facultative parthenogenetic screening method to be used.

PCRs were carried out upon preparations of *D. mercatorum* genomic DNA using general primers (wsp 81F: TGGTCCAA TAAGTGATGAAGAAAC, wsp 691R: AAAAATTAACGCTACTCCA) against Wolbachia and the resulting DNA fragments were subjected to electrophoresis on a 1% agarose gel. The primer sequences and positive control were provided by Julien Martinez.

Selection of *D. mercatorum* strains to sequence

As also seen with other *Drosophila* species,^{16,20,51,89} *D. mercatorum* shows variability in the incidence of facultative parthenogenesis between strains linked to their geographical collection points.^{21,90} In selecting a sexually reproducing strain and a completely parthenogenetic strain of *D. mercatorum* for genomic analysis, we chose one strain from a more ancestral habitat (Brazil) and one from a newly colonized habitat (Hawaii).²⁵ Although changes in gene organization between strains from two distant geographical locations will reflect selection of traits enabling survival in these different environments, it will also maximize the chance of identifying potential genome changes facilitating facultative parthenogenesis.

High molecular weight DNA preparation

The High molecular weight DNA preparation method was a mixed protocol.^{91,92} Flies were homogenized in 150 μ l of SDS buffer (0.5% (w/v) SDS, 0.200 M Tris, 0.25 M EDTA, 0.250 M NaCl) using a handheld electric pestle mixer for 10 seconds. 350 μ l of SDS buffer was added to the mixture and incubated at 37°C for 4 h; then 5 μ l of RNase A (100 mg/ml) was added and incubated at 37°C for 2 h; and then 5 μ l of Proteinase K (20 mg/ml) was added and incubated for a further 2 h at 50°C. The DNA was extracted using 240 μ l of the phenol layer of phenol/chloroform/isoamyl alcohol (25:24:1), Acros Organics from Fisher Scientific. Following gentle mixing for 3 min at room temperature, the mixture was centrifuged at 12,000 x g for 10 min, and the supernatant decanted. The phenol extraction was repeated once more followed by a final chloroform layer extraction. The DNA was precipitated with 500 μ l -20°C absolute ethanol and let stand at -20°C for more than 5 min before removing the DNA precipitate. The DNA was placed into a new tube with 80% ethanol and centrifuged at 12,000 g for 3 min and the pellet washed again with 500 ml of 80% ethanol before centrifugation at 12,000 g for 3 min to remove residual salt. The pellet was then dried at 37°C and 50 μ l of elution buffer (10mM Tris, pH 8.0, in nuclease free water) was added. The DNA was left at room temperature overnight and then at 4°C for a minimum of 2 days prior to sequencing.

Long-read Nanopore library preparation

Parthenogenetic Genome

High molecular weight DNA was extracted from 32 females from an isofemale *D. mercatorum* strain from the Cornell University National *Drosophila* Species Stock Centre (CSC: 15082–1525.07). 457.2 ng of isolated DNA was sequenced on the Nanopore MinION using the SQK LSK-109 ligation protocol and FLO-MIN106D R9 Version Spot-ON Flow Cell RevD.

Sexually Reproducing Genome

High molecular weight DNA was extracted from 32 adult females from the sexually reproducing *Drosophila mercatorum* strain (CSC: 15082–1511.00). A slightly modified QIAGEN Genomic-tip (100/G) protocol was used for library preparation with the following changes: dry frozen flies were homogenized to a fine powder in a tube partially submerged in liquid Nitrogen (N₂). After lysis buffer was added the sample was immediately vortexed for 5 seconds. DNA concentration was quantified using Qubit, Nanodrop, and the Agilent TapeStation. 2.57 μ g and was then sequenced on the Nanopore MinION using the SQK LSK-110 ligation protocol and FLO-MIN106D R9 Version Spot-ON Flow Cell.

Short-read Illumina library preparation

Parthenogenetic Genome

Illumina short-read whole genome sequence data was generated using high molecular weight DNA from a single parthenogenetic female *D. mercatorum*. The DNA was diluted in 52.5 μ l of elution buffer (10mM Tris, PH 8.0, in Nuclease free water) and placed into a Covaris Screw Cap microTUBE for M220 and sonicated using an E220evolution Focused-ultrasonicator. The library was then prepared using the KAPA HyperPrep Kits for NGS DNA Library Prep by Roche and sequenced on a NovaSeq with 150 bp PE reads.

Sexually Reproducing Genome

Illumina short-read whole genome sequence data was generated using high molecular weight DNA from a single sexually reproducing female *D. mercatorum*. The library was then prepared using the NEBNext Ultra II DNA Library Prep Kit for Illumina by New England Biolabs and sequenced on a MiSeq with 150 bp PE reads.

Genome assembly

Polished chromosome-level genome assemblies were created using Oxford Nanopore and Illumina sequencing technology. The genomes of the sexually reproducing and parthenogenetic strains were assembled using wtdbg2 (v2.5)⁶⁸ using the setting “wtdbg2 -x ont -g 200m” and following the consensus generation procedure (wtpoa-cns, minimap2 (v2.24),⁶⁹ samtools⁷⁰) recommended by the author. We then followed a polishing procedure similar to that used in the Vertebrate Genomes Project (VGP), wherein alignments of Illumina reads were compared to the genome assemblies and used as input to freebayes.⁷¹ bcftools consensus (v2.18)⁷² was used to correct the genome to match homozygous calls from the Illumina alignments. The assembly quality assessed using standard metrics of NG50, coverage, and genome size (Figure 1B), all of which indicated that the genome sequences were of similar or greater quality to other de novo *Drosophila* genome assemblies. The apparent larger size of the sexually reproducing genome, which shows high representation of repetitive sequence, likely reflects different DNA preparation methods resulting in the overall size of the contigs (NG50) being larger.

Genome alignment

We aligned the genomes using minimap2 (v2.24) with settings “-a -x ont”, resulting in alignments for each input nanopore read set to its respective assembly. We compared the two *D. mercatorum* assemblies to each other using whole genome alignment with wfmash (v0.6).⁷³ We additionally completed whole genome alignments with wfmash to evaluate the relationship between the assemblies and with the *D. melanogaster* reference assembly, using “wfmash -p 70”. Comparison of the *D. mercatorum* genome assemblies with the *D. melanogaster* reference genome showed the contigs match to single chromosome arms (Figures 1C, S2A, and S2C). There is some overlap between the chromosome arms because centromeres and telomeres are composed of transposable elements in *Drosophila*.^{93–96} There was 75.8% and 75.5% gap-compressed sequence identity (n.b. this metric counts each gap as a single base irrespective of length, as described in <http://lh3.github.io/2018/11/25/on-the-definition-of-sequence-identity>) for the sexually and parthenogenetically reproducing genomes compared to the *D. melanogaster* genome, respectively. The alignment of the sexually reproducing genome covered 75.3 Mbp, while the parthenogenetic genome covered 73.4 Mbp of the *D. melanogaster* reference.

Genome coverage analysis

Evaluation of the coverage of alignments was completed using bedtools (v2.18).⁷⁴ Windows for each 10kb of the assembly were established using “bedtools makewindows”, and in each we computed the coverage of alignment using “bedtools coverage -mean”.

Self-heterozygosity and inter-strain divergence analysis

To establish estimates for pairwise heterozygosity in each strain, we aligned the Illumina data used for polishing back to the assemblies using “bwa mem -t 24”. Normalize them using vcfwave “freebayes -f”, using vcfwave vcfilt -f ‘QUAL > 20’ and measure heterozygosity using bcftools. The sexually reproducing and parthenogenetic *D. mercatorum* genomes were highly similar to each other, having 98.78% gap-compressed sequence identity (Figure 2A). An assembly quality value (QV) metric, based on comparison of 19-mers in the Illumina data to the assemblies, suggest error rates of around 1/1000; the QV for the sexually reproducing *D. mercatorum* genome is 26.545 and 28.6212 for the parthenogenetic *D. mercatorum* genome, which is adequate for our analyses.

We repeated the self-heterozygosity analysis except for each strain we aligned against the other *D. mercatorum* assembly and then called variants. We normalized them using vcfwave, removed low-quality variants with vcfilt -f ‘QUAL > 20’, and then measured the number of non-reference homozygous SNPs (not hets) for the parthenogen compared to the sexually reproducing and divided the number of repeats by the respective genome size to obtain a strain-wise divergence estimate. There were 109035 heterozygous single nucleotide polymorphisms (SNPs) in the sexually reproducing *D. mercatorum* genome, and since the genome is 171182504bp the pairwise heterozygosity is estimated at 0.0637% for SNPs. By contrast, there were 16474 heterozygous SNPs in the parthenogenetic *D. mercatorum* genome, and since the genome is 161570079bp the pairwise heterozygosity is estimated at 0.0102% for SNPs. The genomes contained 0.82%–0.84% SNPs when compared to each other.

Mercury k-mer spectrum analysis

To further evaluate heterozygosity, we explored the k-mer copy spectrum of the assemblies relative to their respective Illumina read sets using meryl (v1.3) and mercury (v1).⁷⁵ There were no duplicated haplotype-specific contigs (Figure S1C). This indicated the absence of any large-scale genome abnormalities in our assemblies.

De novo genome annotation

The genomes were annotated using homology to *D. melanogaster* gene annotations and the annotation was polished using the *D. mercatorum* transcriptome data we produced in this study from Stage 14 egg chambers. To annotate the *D. mercatorum* genome assemblies, we first identified repeats in the genome assembly using RepeatModeler2 (v2.0.1)⁷⁶ with option -LTRStruct. We then soft-masked repeats in the genome utilizing the found repeats using RepeatMasker (v4.0.9)⁷⁷ with options -gccalc -s -nolow -norma -gff -xsmall (or without -xsmall for hard-masked assembly used in nucmer analysis, see above). Next, we trimmed RNA-seq paired-end reads (see differential gene expression analysis below) using cutadapt (v2.0)⁷⁸ and options -a AGATCGGAAGAGC -A AGATCGGAAGAGC -q 20 -minimum-length 50. Trimmed reads were mapped against the unmasked genome assembly using STAR (v2.7.0e)⁷⁹ and bam files from parthenogenic/facultative parthenogenic/sexual strains merged using samtools merge.⁷⁰ To predict genes, we employed

BRAKER2⁸⁰ using the soft-masked genome assembly (with option `–softmasking`) and the merged bam file. To identify most likely 1-to-1 homologs between *D. mercatorum* and *D. melanogaster* genes, we first extracted the CDS sequences from the identified *D. mercatorum* genes using `gffread` and obtained the protein gi numbers from *D. melanogaster* with `esearch` and `efetch` (July 2020). We then used BLASTx (ncbi-blast-2.10.1)⁸¹ to blast the *D. mercatorum* CDS against the *D. melanogaster* proteins with options `-db nr -num_threads 60 -outfmt '6 qseqid stitle qlen slen length qcovs qcovhsp evaluate bitscore pident sacc sseqid sscinames' -max_target_seqs`. The blast output was filtered for entries with an evalue of $<1e-10$, minimum query coverage >50 and percent identity >35 . Gene names and FBgn numbers were added to accession numbers utilizing mappings obtained from FlyBase (fbgn_NAseq_Uniprot_fb_2020_03.tsv). To get reverse hits, we used tBLASTx to blast the *D. melanogaster* CDS (reference version 6.35) against the *D. mercatorum* CDS with the same options as above except from `-max_target_seqs` and filtered the output using the same cut-offs.

The automatic de novo annotations are given in [Data S2](#). The annotations for the list of differentially expressed genes for each dataset needed to be manually curated because they matched multiple genes. The correct annotation was selected by chromosome arm or local synteny ([Data S3A–S3D](#)). When the correct annotation could not be identified then we left all potential annotations listed.

Nucmer and gene distribution analysis

As a complementary approach to the dot plots, we further used nucmer (MUMmer v3.23)⁸² with options `–coords –maxgap 500 –maxmatch` to align contigs from *D. mercatorum* to *D. melanogaster* chromosomes (reference version v6.27). To avoid potential misalignments caused by repeats, both genomes were hard-masked using RepeatMasker⁷⁷ (see annotation below) before running nucmer. The `show-coords` command with `-l -c` option was then used to create a coordinates file. We considered that a *D. mercatorum* contig maps to a *D. melanogaster* chromosome if $>40\%$ of the alignments map to one *D. melanogaster* chromosome, while all other chromosomes have $<20\%$ alignments. The majority of putative genes were distributed evenly on the 14 largest contigs of both sexually reproducing and parthenogenetic genomes ([Figure S1A](#)). The distribution of reads over the assembled genome indicated uniform sequencing coverage across all large contigs, which comprise most of the assembled sequence ([Figure S1B](#)). Any deviations in coverage occur in shorter contigs that may represent mis-assemblies or collapsed repeats.

Genome assembly content

We found that the sexually reproducing genome assembly contained contigs at lower-than-expected coverage, which we believe to be *Acetobacter* DNA. The *D. mercatorum* genomic DNA was prepared from whole animals and therefore included the genome of a commensal gut bacterium, *Acetobacter acetii*, common in *Drosophila* lab stocks.⁹⁷ We manually checked each of the contigs in the size range of those that had lower than expected coverage for both the parthenogenetic and sexually reproducing genome assemblies. There were 31 contigs that contained only *Acetobacter acetii* genomic DNA in the sexually reproducing strain and 6 in the parthenogenetically reproducing strain. Once the contigs containing *Acetobacter* genes were filtered from both genomes, there were a comparable number of putative genes in the sexually reproducing (17,364) and parthenogenetic (17,566) *D. mercatorum* genome assemblies.

BUSCO analysis

BUSCO (v5.3.2)⁸³ was run with options `–m genome` and `–auto-lineage-euk` on the genome assemblies of the parthenogenetic and sexual *D. mercatorum* strains. The *D. melanogaster* genome (v6.27) was included for comparison. The genomes of the sexually reproducing and parthenogenetic strains were 98% and 99% complete, respectively, in comparison to the dipteran specific BUSCO dataset ([Figure S1D](#)). By comparison, the *D. melanogaster* reference genome (release 6) is only 98.7% complete when compared to the dipteran-specific BUSCO dataset. Together these analyses confirmed the expected high divergence between *melanogaster* and *mercatorum* and indicated that the chromosome-level genome assemblies for the sexually and parthenogenetically reproducing *D. mercatorum* strains were suited to comparison with the *D. melanogaster* genome for the purpose of identifying gene homologues for parthenogenesis screening.

Mitotic chromosome preparation

Brains were dissected from 3rd instar larvae in saline (0.7%NaCl), incubated in 0.5% trisodium citrate for 9 min, and fixed for 60s in 45% acetic acid and 5 min in 60% acetic acid on a cover slip. The fixed brains were squashed, frozen in liquid N₂, and the coverslip removed using a scalpel. The preparation was washed for 5 min in 70% and 5 min in 100% ethanol. The slides were baked at 58°C for 1 h in a dry oven and then denatured with 70% formamide in 2×SSC at 70°C for 20 min. Finally, the slides were washed again for 5 min in 70% and 5 min in 100% ethanol and then moved onto the HRC protocol.

Polytene chromosome preparation

Salivary glands were dissected from 3rd instar larvae and prepared for in situ using the protocol available from the Duronio Lab (<https://theduroniolab.web.unc.edu/resources#protocols>). Followed by the HRC protocol.

Molecular Instruments HCR sample preparation

All materials including buffers and probes were purchased or gifted from Molecular Instruments. To ensure optimal hybridization to mitotic chromosome preparations, probes were selected for accessible gene regions by the criteria that the chosen genes were highly transcribed in brain tissue. The standard Molecular Instruments HCR protocol (v3.0) for sample on slide was used.

RNA library preparation

Three strains were used for gene expression analysis: sexually reproducing (CSC: 15082-1511.00), parthenogenetic (CSC: 15082-1525.07), and facultative parthenogenetic (CSC: 15082-1527.03). Three biological replicates of all libraries for each of the three *D. mercatorum* strains were used in this study. All animals for each sample were kept together, controlled for population size while they were developing, and treated identically prior to dissection. The virgin females were stored at 25°C to reach the desired age (3–12 days old) before dissection. Stage 14 egg chambers were dissected 0.1% PBST from all flies on the same day and in batches controlling for time of day. 4 stage 14 egg chambers were taken from the ovaries of 20 flies and individually transferred to a 1.5ml tube containing ice cold 0.1% PBST. Once the target amount was reached, PBST was removed and RNALater solution (200 μ l) was placed into the tube to fix the egg chambers and stabilize the RNA. The tubes were stored at 4°C overnight. The RNALater was removed, and the RNA was prepared using the manufacturer's recommended protocol for the RNeasy kit from Qiagen. Libraries were prepared using the manufacturer's recommended protocol of the KAPA mRNA HyperPrep Kit from Roche. The RNA libraries were sequenced on a NovaSeq with 150 bp PE reads.

Differential gene expression analysis

We used STAR (v2.7.0e) to map trimmed, paired-end reads against the *D. mercatorum* assembly employing the gene annotations (gtf file) created by BRAKER2 (see above) and counted reads mapping to exons using featureCounts (subread v1.6.3).⁸⁴ We filtered out genes that had 0 counts across all samples, and then used DESeq2 fitting 'parthenogenesis condition' as factor and contrasting pairwise expression differences across the three conditions. P values were corrected for multiple testing using FDR.

Gene Ontology (GO) analysis

We performed GO enrichment (Fisher's exact test) and gene set enrichment analysis (GSEA, Kolmogorov-Smirnov test) using the weight01 algorithm in topGO.⁸⁵ As there are no GO annotations available for *D. mercatorum*, we employed the corresponding *D. melanogaster* homologs or orthologs (see above) and therefore assumed that genes would have a similar function and protein sequence in the two species. For *D. mercatorum* genes that mapped to multiple *D. melanogaster* genes, we randomly picked one *D. melanogaster* gene, and accounted for differences in enrichment by performing a total of 100 GO analysis iterations. For each iteration, we considered GO terms significant at an FDR (false discovery rate) <0.1 and report the frequency depicting how often a GO category fell below this FDR threshold. The analysis was performed for all pairwise parthenogenesis-type comparisons, considering either all or only up or downregulated genes.

Drosophila facultative parthenogenesis screen

Since this was the first screen to test the contribution of specific gene variants to parthenogenetic reproductive ability, we needed to benchmark our screening method. Using 13 different *Drosophila* species, we first determined that a baseline indicator of facultative parthenogenesis could be indicated by testing the ability of approximately 500 virgin female flies to generate progeny (Data S4A). Strong levels of facultative parthenogenesis could be detected with as few as 30 flies. Using these criteria, we found that two typical laboratory strains of *D. melanogaster* (*w* and *Oregon-R*) showed no parthenogenesis whatsoever, whereas a strain caught in the wild (*CB1*) produced a small number of embryos that showed restricted development before dying (Data S4B). This accords with previous findings that *D. melanogaster* strains caught in the wild have slight ability to undertake facultative parthenogenesis.²⁰

We tested *D. melanogaster* homologues of genes that had decreased expression in the facultative parthenogenetic and fully parthenogenetic *D. mercatorum* eggs using CRISPR knock-out alleles that we generated (Data S5), publicly available mutant alleles, or established fly stocks carrying RNAi constructs to down-regulate selected genes. The RNAi lines were all previously verified to have no known off-target effects and were published or have a verified phenotype (link to publicly available data provided in Data S6). Phenotypes of the RNAi lines were compared to the phenotype of a published publicly available mutant allele used in this study (Data S6) and/or were compared to the phenotypes of published publicly available alleles used in this study and/or were compared to another independently established fly stock carrying an RNAi construct to down-regulate gene of interest (Data S6).

The facultative parthenogenesis screen was performed on the offspring of females having the exact genotypes given in Data S6A and S6B. Only the genotype of the mother is given, although the mothers themselves arise from crosses that introduce different non-balanced chromosomes. Chromosomes carrying the genes of interest were followed using the following balancer chromosomes: FM6 or FM7 for the X chromosome, CyO or SM5a for the 2nd chromosome, and TM6B, TM6c, or TM3 for the 3rd chromosome. The mothers all have the indicated genotype given for the chromosome of interest and the non-balanced chromosomes arise from differing stocks within our fly collection.

In addition to negative controls for every experiment, there were also control gene variants that were screened in order to determine if non-specific mutations could cause facultative parthenogenesis. We also had controls for the constructs used to drive expression of interfering RNAs and UAS/Gal4 overexpression constructs⁹⁸ used in the study. The following Gal4 drivers for were tested as controls for facultative parthenogenesis: *bag of marbles (bam) gal4*; *maternal tubulin (MTB) gal4* on the 2nd and 3rd chromosomes; and *nanos (nos) gal4*. Both *MTB-gal4* and *nos-gal4* stocks showed a small degree of facultative parthenogenesis. We also screened the double balancer stock that we used to balance any stocks used in our double variant screen. It too showed a low level of facultative parthenogenesis.

Five negative experimental controls were used (last section in Table 1): 1) an allele for *CG3436*, a gene that is expressed in the egg and implicated in cell cycle regulation but not differentially expressed, 2) two alleles for *dhd*, another gene that is necessary for the

onset of embryogenesis, 3) an allele and an RNAi line for *Klp64D*, a gene that is not involved in the cell cycle and not differentially expressed, 4) an allele and an RNAi line for *Trx-2*, a gene that is necessary for the onset of embryogenesis, and 5) an allele and an RNAi line for *white (w)*, which was not expressed in the *D. mercatorum* eggs. There was a low level of facultative parthenogenesis in some of the controls (Data S6A), which we propose may be caused by the *Desat2* allele (see Main Text).

For the single gene variant screen, the control used for the statistical analysis was RNAi stock, the *gal4* stock used in the experiment, the *w⁻* mutant allele, the UAS-line without Gal4 driven expression, or the *pUbg-Rcd4-GFP* stock.⁹⁹ For the double gene variant screen, the control used for the statistical analysis is either given with the experiment Data S6B or it was the strongest single gene variant causing facultative parthenogenesis in the given combination.

We found that the many RNAi lines used in the primary screen had a small degree of facultative parthenogenesis without expression being driven by Gal4. These were the lines for *bam*, CG4496, CG10433, *CRMP*, *Desat2*, *f*, and *FER*, and for the controls *Klp64D* and *w*. In all these cases, the RNAi line had fewer instances of facultative parthenogenesis when crossed to the Gal4 drivers, and thus when the expression of the RNAi was induced. This indicates that the RNAi does not itself cause facultative parthenogenesis but rather it is the result of something in the background of the RNAi stocks.

We tested the notion of a background mutation in the RNAi lines using the *bam* RNAi line. We crossed this line to 8 different *gal4* lines (*bam* (X), *bam* (II), *nos*, *MTB* (I), *MTB* (II), *actin* (*act*), and *ovarian tumour* (*otu*)) and found that some could drive a low level (0.1-0.2%) of facultative parthenogenesis but at levels less than or equal to the RNAi stock alone (0.2%). We also crossed the RNAi line to the *white* mutant allele that we found not to have any degree of facultative parthenogenesis. Finally, we checked that the observed facultative parthenogenesis could not be caused by the RNAi target gene by crossing the *bam* RNAi line to a mutant allele of *bam* and found that this also reduced the level of facultative parthenogenesis. Together, the evidence strongly suggests that the low degree of facultative parthenogenesis is caused by a background mutation: (1) It is not the presence of the RNAi construct since many RNAi lines did not show any parthenogenesis, (2) It is not the expression of the RNAi since driving the expression did not enhance the degree of facultative parthenogenesis. (3) It is not due to the *bam* mutation because crossing the RNAi line to a *bam* null mutant allele did not enhance the degree of facultative parthenogenesis.

The first gene variant for which we observed a reproducible amount of facultative parthenogenesis was the background mutation present in the *bam* RNAi line, that we therefore used as a tool to optimize our experiments. Temperature optimization revealed the highest level of facultative parthenogenesis at 18°C, moderate levels at 25°C, and no parthenogenesis at all at 29°C (Data S6A). We chose 25°C for our subsequent experiments as this would allow them to be completed in approximately 3 months compared to 5 months at 18°C due to the difference in lifespan of the flies at these temperatures.

Desat2 allele screening

PCRs were carried out using genomic DNA preparations of *D. melanogaster* stocks (primers: *Desat2*-UTR-FWD AAGAGC TCGCCAGCTATCTAC and *Desat2*-UTR-REV AAGGACACCCGTTTCTCTGG). The resulting DNA fragments were subject to electrophoresis on a 2% agarose gel, purified, and sequenced and then compared to *D. melanogaster* (assembly Release 6 plus ISO1 MT), which does not have the 16bp deletion 150bp upstream of the start codon.

Second generation facultative parthenogenesis

To determine if it was possible to generate a second generation of facultative parthenogenesis, large numbers of virgins were collected from the three stocks that could generate parthenogenetic animals. The stocks were slightly homozygous viable and hence both heterozygous and homozygous females were screened for facultative parthenogenesis. The shorthand to denote this in the genotype is to put the allele that may or may not be present in brackets ‘’. This is different from the secondary screen, which was not performed on stable stocks. These females were maintained changing the food weekly. The experiments were collapsed into fewer tubes when the flies were past the age when they have peak facultative parthenogenesis, which is after 40 days, or when there were fewer than 20 flies remaining in the tube. The first generation of parthenogens (F1) were then transferred to fresh food and maintained for their life, changing the food weekly. We checked for development of a second generation of facultative parthenogenesis by examining the food, as in the main facultative parthenogenesis assay.

Embryo preparation

Mothers were aged for at least 2 weeks at 25°C prior to initiating embryo collections, a minimum of 3 independent replicates of 200 virgin females were used for these collections. All embryo collections were done in parallel with the controls and under the same conditions. Unfertilized eggs were collected for 2 h at 25°C and then incubated at 25°C for 2 h, 8h, or 18h. Fertilized eggs were collected for 2 h and immediately prepared for fixation. Embryos were dechorionated (50% bleach) for 3min, washed, transferred to either a 50:50 heptane:methanol mixture or a 50:50 heptane:4% paraformaldehyde/PBT mixture, and fixed for 20 min on a rotator. The embryos were washed 3 times with 100% Methanol and then rehydrated. The rehydrated embryos were then washed 2x with PBS containing 1% Tween (PBT), blocked for 1h in PBT containing 10% BSA before and incubated overnight in the primary antibody at 4°C. After washing the embryos 3x10min with PBT the embryos were incubated with the secondary antibody for 4 h at room temperature, washed 3x10min with PBT, and then mounted in Vectashield (Vector) containing DAPI to visualize DNA.

Primary antibodies

Mouse α -acetylated-Tubulin antibody, clone 6-11B-1 (1:200 dilution), mouse α -Tubulin antibody, DM1A (1:200 dilution), rabbit α -Histone H2A antibody, ab13923 (1:500 dilution), rabbit α -Cnn antibody, Glover lab (1:200 dilution).

Secondary antibodies

(all 1:500 dilutions) Goat α -Mouse 488 and 647 from Life Technologies, Goat α -Rabbit 488 from Invitrogen and 647 from Life Technologies.

Imaging

All images were acquired on a Leica SP8 confocal microscope, and the images were minimally optimized for brightness and contrast using ImageJ (Fiji).⁸⁶ No other image alteration was performed. All images presented are projections of multiple focal planes.

QUANTIFICATION AND STATISTICAL ANALYSIS

The information on the statistical tests is provided in the figure legends or in [Data S2](#) and [S3](#). The n numbers were counting cells for the mitotic karyotyping experiments, individual embryos for the embryo experiments, or animals for the final karyotype experiments. The Fisher's Exact Test (in R) was used for the functional screens and for the parthenogenetic embryo analysis. It was chosen because it is permissive to having samples with '0' instances of positive cases in the controls. For the GO enrichment the Fisher's exact test was used and for the gene set enrichment analysis the GSEA, Kolmogorov-Smirnov test was used.